REOXIDATION KINETICS OF FLASH REDUCED IRON PARTICLES RELEVANT TO A NOVEL FLASH IRONMAKING PROCESS

by

Zhixue Yuan

A thesis submitted to the faculty of
The University of Utah
in partial fulfillment of the requirements for the degree of

Master of Science

Department of Metallurgical Engineering

University of Utah

December 2013

The University of Utah Graduate School

STATEMENT OF THESIS APPROVAL

The thesis of **Zhixue Yuan**

has been approved by the following supervisory committee members:

Hong Yong Sohn	, Chair	**07/03/2013** Date Approved
Zhigang Zak Fang	, Member	**07/03/2013** Date Approved
Michael L. Free	, Member	**07/03/2013** Date Approved

and by **Manoranjan Misra** , Chair of

the Department of **Metallurgical Engineering**

and by David B. Kieda, Dean of The Graduate School.

ABSTRACT

A novel flash ironmaking process based on hydrogen containing reduction gases is under development at the University of Utah. This process will directly reduce fine iron oxide concentrate particles in suspension in a flash reactor. The goal of this work was to study the possibility of reoxidation of iron particles in various gas mixtures from the kinetic point of view. The last stage of hydrogen reduction of iron oxide, i.e., the reduction of wustite, is limited by equilibrium. As the gas particle mixture cools down in the lower part of the flash reactor, the reoxidation of iron could take place because of the decreasing equilibrium constant and the high reactivity of the freshly reduced fine iron particles. The effects of temperature (823 – 973 K) and H_2O partial pressure (40 – 100 pct.) on the reoxidation rate were examined. The nucleation and growth model was shown to best describe the reoxidation kinetics. Pressure dependence is first order with respect to water vapor, and the activation energy is 146 kJ/mol. A complete rate equation that adequately represents the experimental data was developed. For oxidation in O_2-N_2 gas mixtures, effects of temperature (673 – 873 K) and O_2 partial pressure (5 – 21 pct.) were studied and the nucleation and growth model was used to describe the initial period of oxidation. Pressure dependence is first order with respect to oxygen and the activation

energy is 14.4 kJ/mol. The oxidation in pure CO_2 gas was investigated in the temperature range of 873 – 1073 K and the results imply that the oxidation will be negligible in the flash reduction process where CO_2 from partial combustion of natural gas with oxygen accounts for less than 10% in the gas mixture.

TABLE OF CONTENTS

ACKNOWLEDGMENTS

I would like to express my profound gratitude to my advisor, Professor Hong Yong Sohn, whose enormous technical expertise, tireless work ethic, and positive life attitude have inspired and motivated me as a young researcher over my graduate years. And his great professionalism will continue to spur me throughout my professional career as a metallurgist.

I would like to thank my thesis committee professors, Professor Zhigang Zak Fang and Professor Michael Free, for their time and effort in reviewing my work.

A great deal of thanks is due to Dr. Moo Eob Choi and Mr. Miguel Olivas-Martinez for their generous instructions and helpful technical discussions during my research.

The financial support from American Iron and Steel Institute (AISI) through a Research Service Agreement with the University of Utah under AISI's CO_2 Breakthrough Program is acknowledged. This material also contains results of work supported by the U.S. Department of Energy under Award Number DE-EE0005751.

Special gratitude is extended to my best friend and beloved girlfriend, Jingzhu 'April' Li, who always cares about and believes in me. I would not be where I am today without her consistent encouragement, trust, and love.

Disclaimer: This report was prepared as an account of work sponsored by an agency of the United States Government. Neither the United States Government nor any agency thereof, nor any of their employees, makes any warranty, express or implied, or assumes any legal liability or responsibility for the accuracy, completeness, or usefulness of any information, apparatus, product, or process disclosed, or represents that its use would not infringe upon privately owned rights. Reference herein to any specific commercial product, process, or service by trade name, trademark, manufacturer, or otherwise does not necessarily constitute or imply its endorsement, recommendation, or favoring by the United States Government or any agency thereof. The views and opinions of authors expressed herein do not necessarily state or reflect those of the United States Government or any agency thereof.

CHAPTER 1

INTRODUCTION

1.1 Description of the Flash Ironmaking Process

A novel flash ironmaking process is currently under development at the University of Utah as a promising alternative ironmaking process that would greatly reduce CO_2 emissions and energy requirement compared with ironmaking in a blast furnace.[1-3] In this process, pure H_2 would be the most attractive reducing agent, although other H_2 containing gases such as natural gas or syngas could also be used.[3]

In the temperature range of 1500 – 1900 K expected in the flash reduction process, H_2 is the main reductant even if CO may be present when gases from hydrocarbon fuel resources are used. Fine iron ore concentrate particles will be directly fed into the flash reactor. The reduction reactions take place in a suspension status, which allows less than ten seconds residence time of concentrate particles.[4,5] This novel process is similar to flash smelting in copper production industry in terms of reactor type, shown in Figure 1.[6-8] However, it has some essential differences from copper sulfide flash smelting, listed in Table 1.[9]

The overall reaction of the reduction of magnetite by hydrogen is

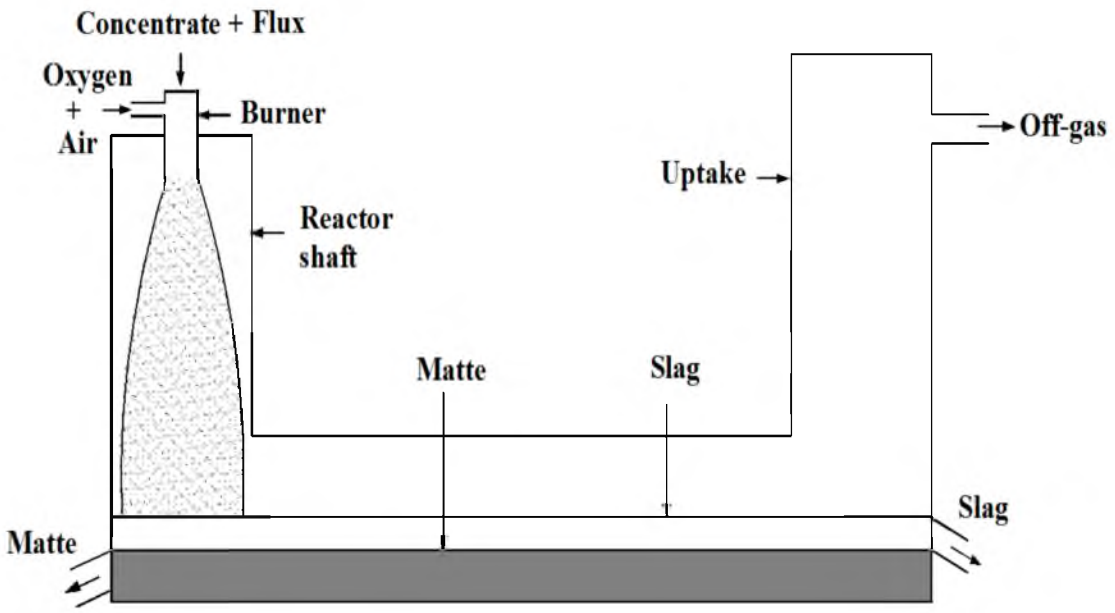

Fig. 1 Schematic diagram of an Outokumpu flash furnace for copper sulfide smelting

Table 1. Comparison between copper sulfide flash smelting and novel flash ironmaking

Parameters	Copper Sulfide Flash Smelting	Novel Flash Ironmaking
Reaction Heat	Exothermic	Endothermic
Reaction Reversibility	Irreversible	Equilibrium limited
Gas Emission	Toxic & More Corrosive Off gas (SO_2)	Combustible & Less Corrosive Off gas (H_2O)

$$H_2 + Fe_3O_4 = Fe + H_2O(g) \quad (1)$$

which consists of the reduction of magnetite to wustite and wustite to metallic iron.

$$H_2 + Fe_3O_4 = 3FeO + H_2O(g) \quad (2)$$

$$H_2 + FeO = Fe + H_2O(g) \quad (3)$$

Reaction 2 has a large equilibrium constant, meaning the reaction is favorable in the forward direction and the equilibrium gas mixture contains little hydrogen. However, reaction 3 is substantially limited by equilibrium, which means the equilibrium gas mixture contains a significant amount of unreacted hydrogen. For example, at 1673 K (1400 °C) the equilibrium gas mixture contains about equal amounts of H_2 and H_2O, shown below:

$$FeO + H_2 = Fe + H_2O(g) \quad K = 0.97 \quad (4)$$

$$\left[p_{H_2O} / \left(p_{H_2O} + p_{H_2}\right)\right]_{eq} = 0.49 \quad (5)$$

This requires the reaction to be carried out in an excess amount of hydrogen to drive the reaction forward. The equilibrium gas composition over a wide temperature range was calculated with the Outokumpu's HSC software.[10] Figure 2 shows the equilibrium gas composition over a wide temperature range and also indicates the possibility of reoxidation as the reaction mixture cools down. Thus the reoxidation kinetics of reduced iron particles is of concern. This is a simplified equilibrium diagram without considering the nonstoichiometric nature of wustite. This does not present a critical problem as far as the process is concerned, because the equilibrium constant of the reduction reaction quite close whether FeO or $Fe_{0.947}O$, representing a wide range of nonstoichiometry, is

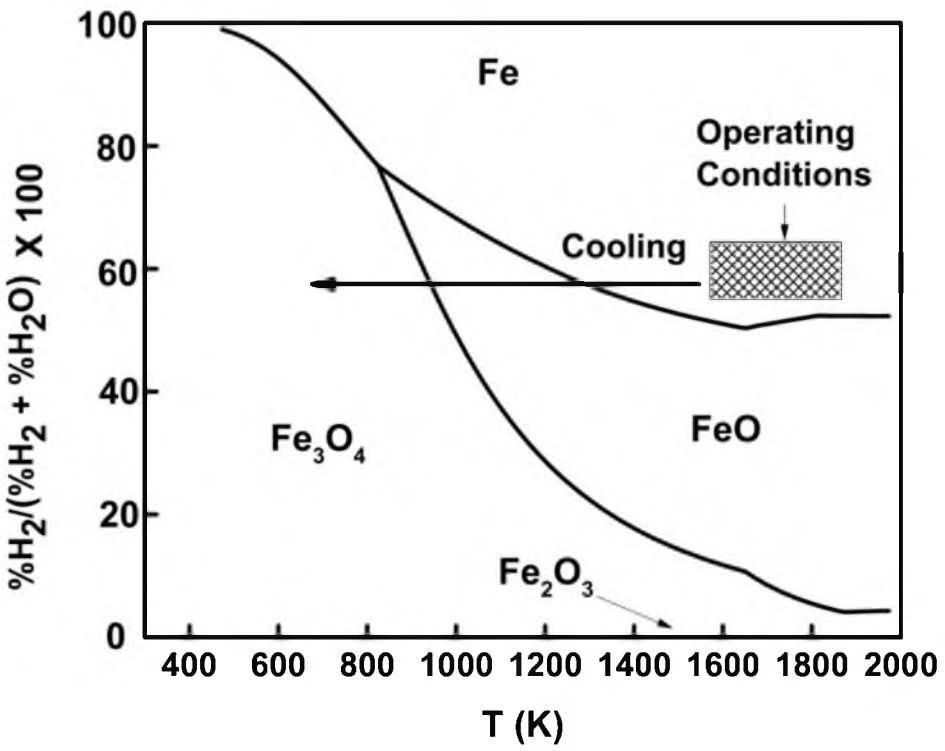

Fig. 2 Equilibrium gas composition versus temperature for the iron-hydrogen-oxygen system

used as the reactant.

Iron product in the novel flash ironmaking process may also come into contact with air at moderate temperatures during transportation. Since direct reduced iron is usually pyrophoric and may ignite spontaneously due to the exothermic oxidation reaction,[11] reoxidation of flash reduced iron particles in O_2-N_2 gas mixtures is also of interest. Since CO from the partial combustion of natural gas and syngas can be available as reducing agent in the novel flash ironmaking process, and the reduction of wustite by CO has an even smaller equilibrium constant than H_2 at the proposed process temperatures, a gas mixture of CO and CO_2 could be present as an oxidizing atmosphere in the flash reactor and thus oxidation tests of the flash reduced iron by CO_2 were also carried out.

1.2 Literature Review on the Oxidation of Iron

Turkdogan *et al.*[12] reported the rate of oxidation to wustite of purified iron strips in water vapor hydrogen gas mixtures in the temperature range of 1123 - 1423 K (850 -1150 °C). In the early stages of oxidation, when the oxide layer is very thin, the rate is controlled by an oxide gas phase boundary reaction, represented by

$$\left(\frac{dn}{dt}\right)_0 = k''\left(1-\frac{1}{a_0''}\right)p_{H_2O} \qquad (6)$$

where k'' is the rate constant, and a_0'', oxygen activity at the surface of wustite in equilibrium with the gas phase, is a function of temperature and oxygen potential of gas mixture. Activation energy for the oxide gas boundary reaction is 80 kJ/g.atom of O. At later stages of oxidation, diffusion in wustite was shown to play a major role in

controlling the oxidation rate. The rate of this stage obeys a parabolic law, represented by the expression

$$m^2 = k_p t + I \tag{7}$$

where m is the gain in weight per unit area, k_p is the rate constant, I is a constant for a particular experiment. The measured parabolic rates were in good agreement with those calculated from the available self-diffusivity of iron in wustite layer.

Yin *et al.*[13] studied the effects of water vapor and oxygen partial pressures on steel of low carbon and low silicon at temperatures of 1173 - 1273 K (900 – 1000 °C) in flowing N_2-H_2-H_2O gas mixtures in which oxygen and water vapor partial pressures were varied independently. The growth kinetics of wustite scale was found to be parabolic after an initial period of linear reaction.

$$\left(\Delta w / A\right)^2 = 2k_w t + C \tag{8}$$

where $\Delta w / A$ is the weight change per unit surface area reached in time, t, k_w the parabolic rate constant and C another constant.

Gas composition dependence of steel oxidation in H_2/H_2O mixtures was interpreted using point defect model involving formation of hydroxyl species on anion sites as well as cation vacancies and formulated as

$$k_w = 0.5 \cdot n\alpha D_v \left(p_{O_2}^{''\,1/n} - p_{O_2}^{'\,1/n}\right) + 2\beta D_{OH} \left(p_{H_2O}^{''\,1/2} - p_{H_2O}^{'\,1/2}\right) \tag{9}$$

where D_v and D_{OH} are, respectively, the diffusion coefficients of vacancy and hydroxyl, p'' and p' are, respectively, the partial pressures at wustite/gas and substrate/wustite interfaces, and α, β are temperature dependent constants. Thus wustite scale growth

on steel in H_2/H_2O gas mixtures is supported by the simultaneous diffusion of iron via cation vacancies and oxygen via substitutional hydroxide species on the anion sublattice.

El-Geassy[14] studied the kinetics and mechanism of the reoxidation of freshly reduced iron compacts in dry air at 473 – 1073 K. Sponge iron compacts were produced by the reduction of iron ore compacts with hydrogen at 1273 K. Weight changes in the reoxidation experiments were determined by an automatic weight recording balance connected to an electronic control unit. It was found that the initial stage of reoxidation followed a linear rate equation of the form:

$$W = K_1 + K_2 t \qquad (10)$$

where W is the reoxidation percent (= 100 × weight gain/weight of oxygen removed from iron oxides by reduction), K_1 and K_2 are constants and t is time of reoxidation. This means the interfacial chemical reaction was the main rate controlling mechanism at the onset of reoxidation process. At the intermediate reoxidation stages, the rate was represented by a parabolic expression of the form:

$$W^2 = K_3 + K_4 t \qquad (11)$$

where K_3 and K_4 are constants, indicating a solid state diffusion rate controlling mechanism. On the other hand, the rate controlling step at the last stage of reoxidation was solid state diffusion in which cavities formed at the interfaces between the oxide films and retained metallic iron grains, with the rate following a logarithmic expression of the form:

$$W = K_5 + K_6 Ln(t) \qquad (12)$$

where K_5 and K_6 are constants.

Bandopadhyay, Ganguly, *et al.*[15-18] performed thermogravimetric studies on the isothermal reoxidation of direct reduced iron in dry air at 720 - 870 K. Sponge iron samples were produced by coal reduction at a rotary kiln pilot plant and were in small pieces, about 500 mg each. The experimental setup consisted of a vertical furnace, a ceramic tube reaction chamber with a sample holder, gas inlet pipe, thermocouples, and a continuous weight recording system. Passivation was observed at the later stages of reoxidation and was believed to be caused by the pore blockage resulting from the iron oxides products. The reoxidation rate was determined to follow a first order law which was expressed in the form:

$$d\alpha / dt = \kappa(1-\alpha) \tag{13}$$

where α is fractional conversion in time t (= weight gain/amount of oxygen required for conversion to Fe_2O_3). It was also pointed out that the reaction rate was proportional to the available surface, which in turn was in a linear relationship with the amount of open pores available in the sponge iron sample. Activation energy of the process was obtained around 56 kJ/mol.

Kaushik and Fruehan[19, 20] studied the oxidation of direct reduced iron (DRI) in CO_2 in a temperature range of 673 - 1173 K (400 to 900 °C). Iron ore pellets were reduced by natural gas to produce DRI samples, in which cracks formed on their surfaces caused by the swelling during reduction. The weight changes of the DRI samples during experiments were continuously measured in a thermogravimetric analyzer (TGA). It was

found that the initial reoxidation rate was controlled by the combination of gas diffusion in pore walls of iron oxides at the outer surface and surface reaction. As the reoxidation proceeded and the oxides layer built up, pore diffusion of gaseous reactant dominated the reoxidation rate, which was confirmed by the rate following linear plots in the final stages of reoxidation.

$$1-2/3\cdot F-\left(1-F\right)^{2/3} : t \qquad (14)$$

where F is the fraction of metallic iron oxidized (= amount of oxygen gained during oxidation/amount of oxygen required to convert metallic iron completely to Fe_3O_4) and t is the reaction time.

1.3 Research Objectives

The literature review revealed that most previous studies were done using iron strips or DRI pellets and DRI samples were produced by coal or natural gas at temperatures lower than 1273 K, which are much lower than the proposed temperature range of 1500 – 1900 K in the novel flash ironmaking process. Moreover, there is a lack of reoxidation data on iron in the form of particles, which have very different morphologies from pellets and strips. Therefore, it is necessary to examine the reoxidation kinetics of flash reduced iron particles in conditions relevant to the novel ironmaking process. References above have shown direct reduced iron (or sponge iron) of large specific surface area, typically around 1000 m^2/kg, can be reoxidized in air quite rapidly.[14,15,21] Although flash reduced iron has a lower specific surface area, 195 m^2/kg (measured by Micromeritics ASAP

2020 in this work), because the process uses a higher reduction temperature than in typical direct reduction processes, the possibility of its reoxidation must be addressed.

In this research, reoxidation of flash reduced iron in H_2O-H_2 gas mixtures was carried out in the temperature range of 823 - 973 K (550 - 700 °C) that is expected to be most important in terms of the thermodynamics and kinetics of the flash reduction process. Gaseous mixtures with 40 - 100 pct. H_2O were tested to determine the dependence of reoxidation rate on the partial pressure of H_2O (the atmospheric pressure in Salt Lake City = 86.1 kPa). Reoxidation of flash reduced iron particles in O_2-N_2 gas mixtures was carried out in the temperature range of 673 - 873 K (400 - 600 °C) and O_2 concentration was varied from 5 – 21 pct. (P_{total} = 86.1 kPa). Rate equations that include related parameters were to be formulated.

As reported by Kaushik and Fruehan,[19,20] the fraction oxidized of DRI pellets in CO_2 can reach 50% at their highest temperature, 1173 K (900 °C), within 25 minutes in a 100 pct CO_2 atmosphere. In the novel ironmaking process, however, CO_2 accounts for less than 10% in the gas mixture produced by partial combustion of natural gas, especially in the presence of a higher CO partial pressure, and the temperatures at which reoxidation would be of concern is much lower. Therefore, CO_2 reoxidation of Fe in flash ironmaking is expected to be much less significant. Nevertheless, reoxidation of flash reduced iron in CO_2 at temperatures of 873 – 1073 K (600 – 800 °C) was studied.

CHAPTER 2

EXPERIMENTAL WORK

2.1 Experimental Apparatus

2.1.1 Horizontal Bifurnace System for Reoxidation in H_2-H_2O Gas Mixtures

Figure 3 shows the furnace system used in this work; it is comprised of two electric furnaces, a gas and deionized water delivery unit and a gas scrubbing unit. The tubing between Furnace 1 (steam generator) and Furnace 2 was wrapped with heating tapes to keep the water vapor from condensing. A peristaltic pump was used to deliver small flow rates of liquid water required by the experiments. Temperature was stabilized for each furnace by an external power controller and was monitored by calibrated K type thermocouples. The tubular reactors (2.54 cm inner diameter) for both furnaces were made of stainless steel, which allowed rapid heating and cooling. Alumina trays (8 cm length, 1.2 cm width, 1 cm depth) were used as sample holders. In order to reduce the diffusion effect from the gas bulk to the particle surface, baked kaowool was placed in the sample trays to raise the sample to the brim of the tray. Blank experiments with $H_2O(g)$ and N_2 indicated that weight changes in the kaowool and sample tray before and after heating were negligible. It has been verified that in the experiment the kaowool bed

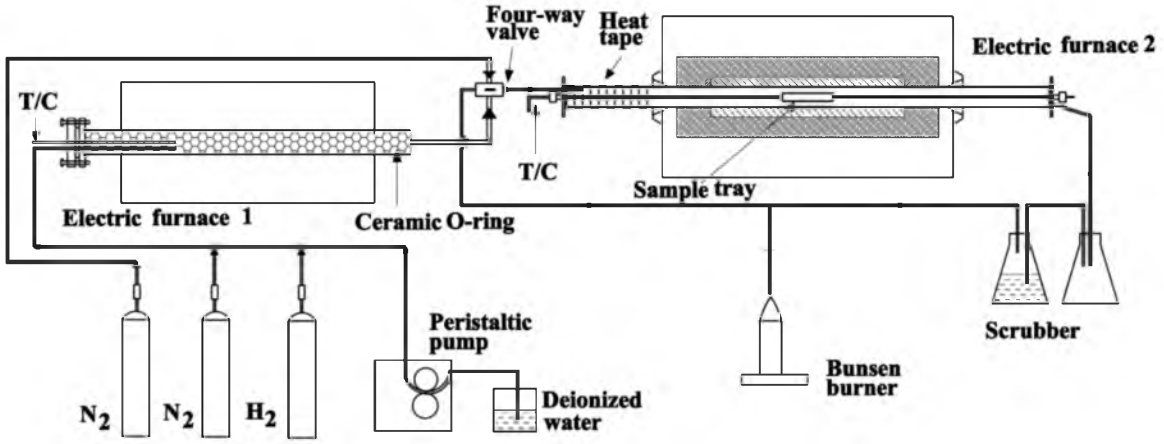

Fig. 3 Schematic diagram of the high temperature furnace system.

was compact enough that the iron particles can stay on it without falling into the gaps in the kaowool. Temperature profile inside Furnace 2 was meticulously measured and the sample tray was placed in the uniform temperature zone with $\pm$ 5 K variation. The difference in reoxidation degree caused by this temperature variation was within $\pm$ 3 pct calculated from the rate equation developed below in this research.

2.1.2 Thermogravimetric Analysis System for Reoxidation in O_2-N_2 and CO_2

A typical thermogravimetric analysis (TGA) unit, shown in Figure 4, was used to measure the oxidation rates in O_2-N_2 gas mixtures and pure CO_2. The system mainly consists of a vertical high temperature furnace and a Cahn balance (model D-101, 1 μg maximum sensitivity), which continuously records weight change during the experiment. To avoid the effect of mass transfer on the measured rates, the sample particles were sprinkled thinly on top of kaowool bed packed to close to the top of a cylindrical sample holder (2.1 cm inner diameter), held in a basket made of chromel wire (resistant to high temperature oxidation and corrosion) and suspended by a platinum wire from one arm of the Cahn electrobalance. The basket was located in a tubular quartz reactor (4.2 cm inner diameter and 111 cm length).

2.2 Materials

Iron ore concentrate from ArcelorMittal (East Chicago, Indiana, U.S.A) was used as the raw material to produce metallic iron particles at 1473 K (1200 °C) and 1623 K (1350 °C) in a drop tube reactor, as described elsewhere.[22,23] The chemical composition

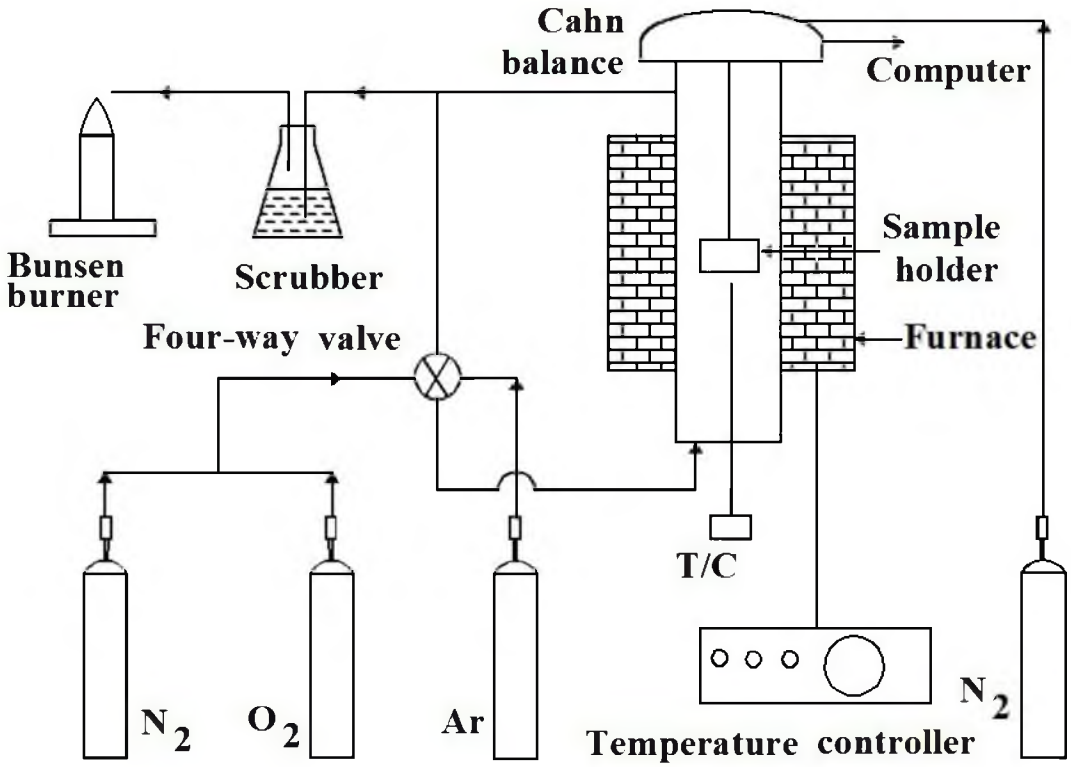

Fig. 4 Schematic diagram of the TGA system.

of the concentrate is presented in Table 2. The reduced iron particles used in the reoxidation experiments had a reduction degree higher than 95 pct. Figure 5 is the XRD pattern of reduced iron particles, showing only iron and impurity silica phases present. Figure 6 shows typical iron particles and the particle size distribution analyzed by processing SEM micrographs. Iron particles were spread isolated on a substrate and SEM micrographs were taken. An image processing and analysis software "IMAGE J" was used to analyze the SEM pictures, which measured the projected area of the particles and back calculated the average diameter of iron particles with the assumption that these irregular particles were spherical. The analyzed SEM pictures contained around 500 particles and the size distribution is over 3 μm interval. The mean particle diameter was 17.5 μm.

Reactant gases (H_2, O_2, N_2, CO_2) used in this research had a minimum purity of 99.95 pct, and thus the impurity level therein was well within the ± 3 pct error range determined later. Water vapor was produced by vaporizing deionized water delivered by a peristaltic pump in the steam generator.

2.3 Selected Range of Conditions

The time the particles spend in the shaft of the flash reactor is very short, measured in seconds, and an actual operation would be carried out under a condition in which the gas phase would still be reducing at or near the operating temperature. Furthermore, the observation during the flash reduction experiments indicated that the extent of

Table 2. Chemical composition of iron ore concentrate from ArcelorMittal.

Component	Wt.%
Total Fe	68.2
FeO	28.2
SiO_2	4.3
CaO	0.19
MgO	0.29
Al_2O_3	0.061
TiO_2	0.021
MnO	0.021
Na_2O	0.011
K_2O	0.044
P	0.014
S	0.0005

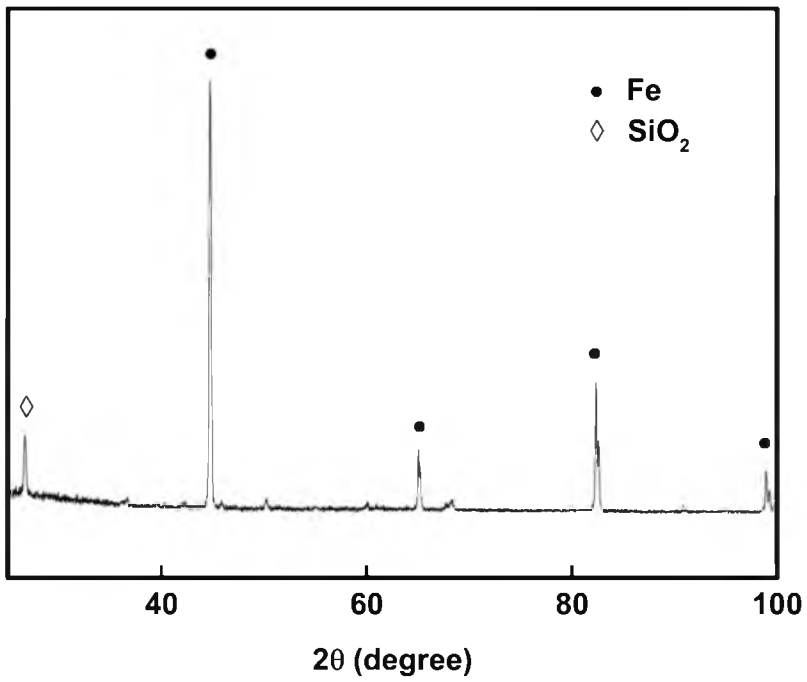

Fig. 5 X-ray diffraction pattern of reduced iron particle, 96% reduction degree at 1623 K

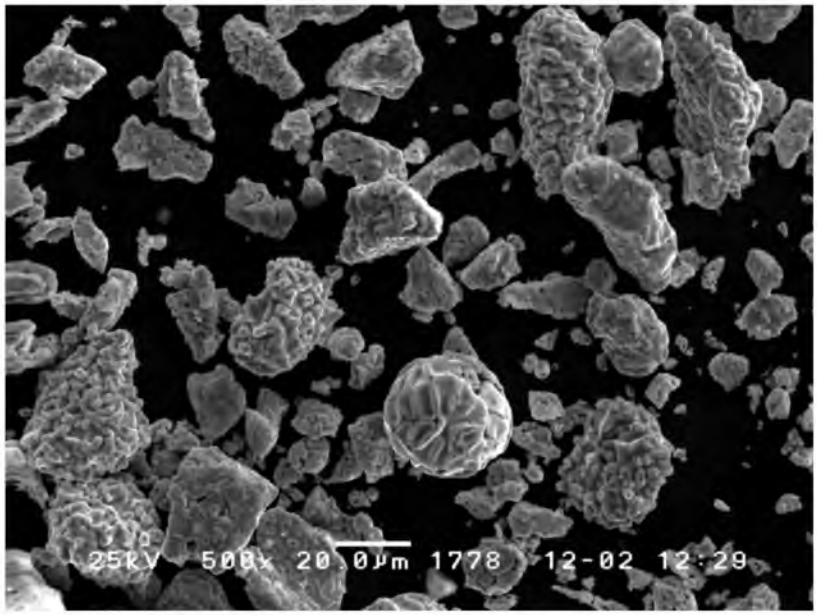

a) typical iron particles

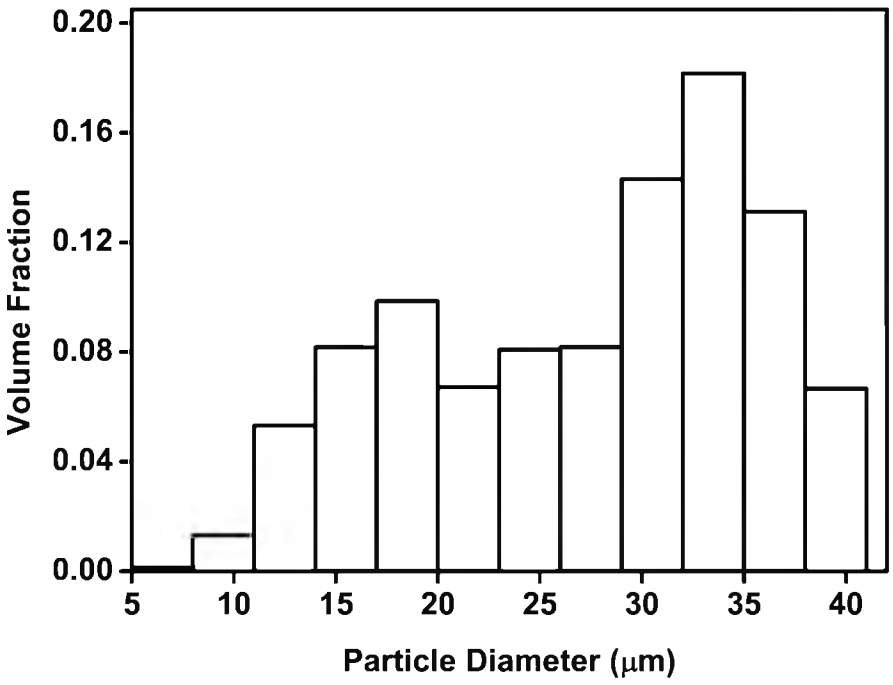

b) particle size distribution

Fig. 6 Particle size distribution of iron particles used in the reoxidation experiments

reoxidation of the reduced iron particles as the gas particle mixture cools down, even when the conditions became thermodynamically feasible, was rather low within the typical residence time of particle flight. Thus, the possibility of reoxidation during the flight is not of great concern. The main concern is the possibility of reoxidation in the particle collector in which the reduced iron will have cooled down significantly and may spend a much longer time.

Our objective here was to generate a database over a wider range of conditions; the cooling conditions would only cover a narrow range of conditions, which would be a specific case of the range covered in this work. Furthermore, the operating conditions can vary. With the database generated in this work, one can compute the possibility of reoxidation under a wide range of operation.

2.4 Experimental Procedure

2.4.1 Reoxidation in H_2-H_2O Mixtures

Iron particles were produced by reducing fine magnetite concentrate particles with hydrogen in a drop tube reactor at 1623 K (1350 °C); the reactions took place in suspension. The reduced iron particles were analyzed by titration to obtain the composition.[24] About 100 mg of these iron particles were sprinkled thinly on top of the kaowool bed in a sample tray in order to eliminate the interparticle diffusion effect of the reactant gas and thus determine the true particle reaction kinetics. After the furnace system was purged by nitrogen and the temperature was stabilized at the target value, the

sample tray was placed in the predetermined uniform temperature zone of Furnace 2. The experiment was started by turning the four way valve to let the mixture of H_2 and $H_2O(g)$ enter Furnace 2. During the experiment, a hydrogen detector was employed to constantly search for hydrogen leaks. Once the experiment was finished, the reactive gases were shut off and N_2 was flowed to purge the system, and the sample tray was unloaded to cool in a closed and dry container. The weight gain caused by reoxidation was then measured. Weight changes related to the volatile components such as sulfur and phosphorus were negligible because of their small contents, as presented in Table 2, which was further confirmed by the negligible weight loss after heating the starting sample in an inert atmosphere.

2.4.2 Reoxidation in O_2-N_2 Mixtures and CO_2

About 120 mg of iron particles flash reduced by H_2 at 1623 K (1350 °C) were sprinkled thinly on the kaowool bed in a cylindrical sample holder, which was then loaded in the chromel basket and suspended in the quartz tube by a platinum wire. The system was then heated up to the experimental temperature in argon atmosphere. N_2-O_2 gas mixtures or pure CO_2 were introduced to the system by switching the four way valve to start the experiment. Once the experiment was finished, the reactor was purged by argon until room temperature and the sample was unloaded and stored in a closed container.

2.4.3 Sample Characterization

Microstructures of the samples were characterized by an FEI NanoNova Scanning Electron Microscope (SEM) (Hillsboro, Oregon), with high resolution mode (immersion mode) off, because the powerful magnetic field at the end of the SEM column can lift a lump of magnetic iron particles and cause it to crash into the SEM column. A TOPCON SM-300 Scanning Electron Microscopy (Oakland, New Jersey) was also employed for some microstructure analysis. XRD analysis was carried out with Philips X' pert X-ray diffractometer with Cu-Kα source 40 kV.

2.5 Definition of Parameters

The reoxidation degree was defined by other researchers as: [14,15,19]

$$\alpha = \frac{\text{Amount of oxygen gained by reoxidation}}{\text{Amount of oxygen required to convert Fe (and FeO) to Fe3O4 (or Fe2O3)}} \tag{15}$$

regardless of the amount of oxygen contained in the starting sample.

With this definition, comparison of the oxidation rates of samples with different initial oxygen contents may be inconsistent. Thus, in this study the reoxidation degree was defined by the fractional oxygen content relative to Fe_xO_y, given by:

$$F = \left(\Delta m + m_0\right) / \Delta m_{Fe-Fe_xO_y} \tag{16}$$

in which Δm is the weight gain caused by reoxidation, m_0 is the weight of oxygen in the starting sample, and $\Delta m_{Fe-Fe_xO_y}$ is the weight of oxygen in Fe_xO_y if all Fe in the starting sample is present as Fe_xO_y. For oxidation of iron in H_2-H_2O gas mixtures and CO_2, Fe_xO_y is Fe_3O_4, while for oxidation in O_2-N_2 mixtures, Fe_xO_y is Fe_2O_3. The reason

for this definition is because at the appropriate temperature and in the H_2O partial pressure ranges, Fe could only be oxidized up to Fe_3O_4, as shown in Figure 2. This was also confirmed by the XRD pattern in Figure 7; whereas for oxidation of iron in O_2, the equilibrium partial pressure of oxygen for reaction (17) is very low. For example at T = 600 °C, p_{O_2} at equilibrium is 4×10^{-14} *atm*, and the oxygen partial pressure in the experiments was significantly higher than the equilibrium one, and therefore the final oxide product was hematite, as also confirmed by the XRD pattern in Figure 8.

$$4Fe_3O_4 + O_2 = 6Fe_2O_3 \quad (17)$$

$$K = 1/p_{O_2} = 2.5\times10^{13} \quad (18)$$

Although in pure CO_2 hematite is formed, magnetite is believed to be the dominant iron oxide present[19], confirmed by the strong magnetite peak intensities in the XRD pattern in Figure 9. Furthermore, from the phase diagram of Fe-C-O,[25] the area of conditions for hematite formation is very narrow, while in the kinetics study most selected conditions are favorable for magnetite. Thus in the definition magnetite is used as the final product.

In H_2-H_2O and CO_2, the oxidation of iron to wustite [or magnetite below 833 K (560 °C)] was the dominant reaction investigated, because: the reactions are equilibrium limited; the reoxidation of iron to wustite accounts for around 75% of the complete reoxidation process; and the early part of reoxidation is of significance as far as an ironmaking process is concerned. In O_2-N_2, however, the reaction studied was the oxidation of iron to hematite because of the large equilibrium constant for oxidation of iron in O_2, as presented by Eq. (18).

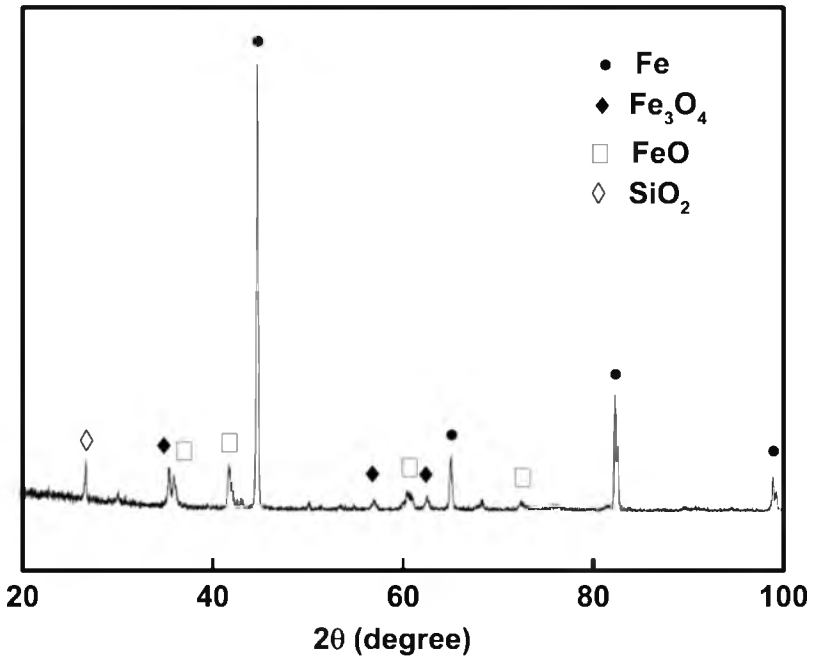

Fig. 7 X-ray diffraction pattern of oxidized iron particles, p_{H_2O} / p_{H_2} = 80%/20% at 873 K (600 °C), P_{total} = 86.1 kPa

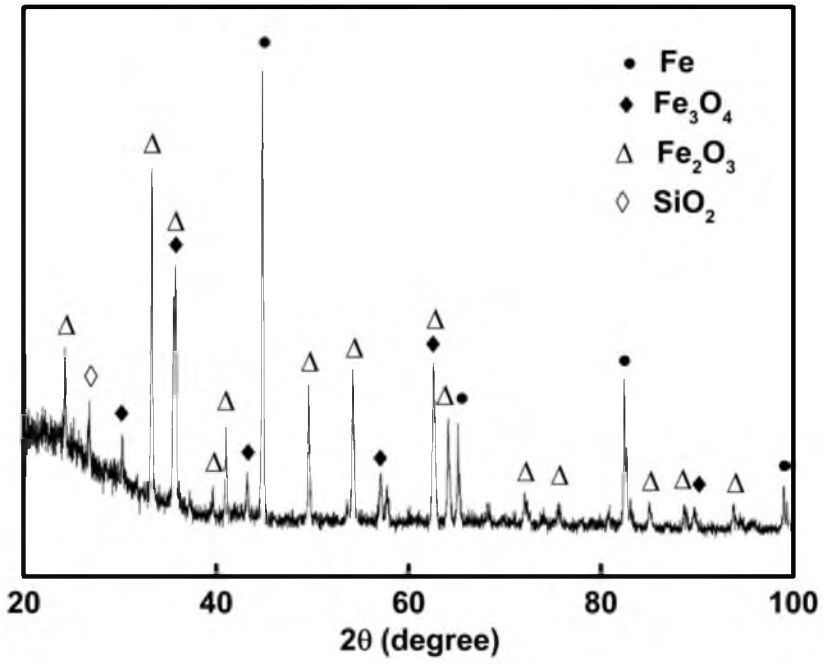

Fig. 8 X-ray diffraction pattern of oxidized iron particles, p_{O_2} / p_{N_2} = 21%/79% at 873 K (600 °C), P_{total} = 86.1 kPa

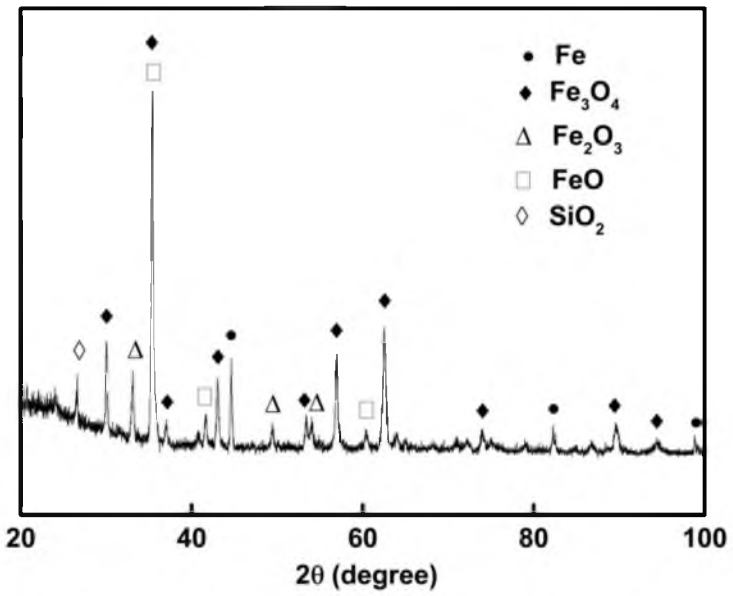

Fig. 9 X-ray diffraction pattern of oxidized iron particles, in pure CO_2 at 873 K (600 °C), P_{total} = 86.1 kPa

With this definition, F does not necessarily start from zero and a direct comparison can be made between the reoxidation rates of samples containing different initial levels of oxygen. In this research, however, the initial oxygen contents of the starting samples were relatively small and this distinction had only a small effect.

CHAPTER 3

EXPERIMENTAL RESULTS AND DISCUSSION

3.1 Reoxidation in H_2-H_2O Gas Mixtures

3.1.1 Elimination of Mass Transfer Effects

Different gas flow rates were tested at 923 K (650 °C) with a fixed sample size of 100 ± 5 mg and constant H_2O concentration of 80 pct. (P_{total} = 86.1 *kPa*). Figure 10 shows that the reaction rate was independent of gas flow rate in the range tested. Therefore, the flow rate of the gas mixture was maintained at 6 L/min at experimental temperatures in the subsequent runs to ensure the elimination of the external mass transfer effect. This is also supported by the calculation of external mass transfer rate (see appendix A).

The effect of interparticle diffusion of gaseous species was eliminated by using a thin sample layer with loosely scattered particles. The area and thickness of iron particles layer were, respectively, 9 cm^2 and 0.5 mm. Calculations (see details in appendix B) showed that at 873 K (600 °C) with 80 pct H_2O(g) the reoxidation would reach completion in 0.13 seconds when the thickness of the sample was 0.5 mm, assuming the reaction was under conditions of interparticle diffusion control.[26] However, this was much faster than the observed rates in experiments, indicating that the reaction was not affected by interparticle diffusion.

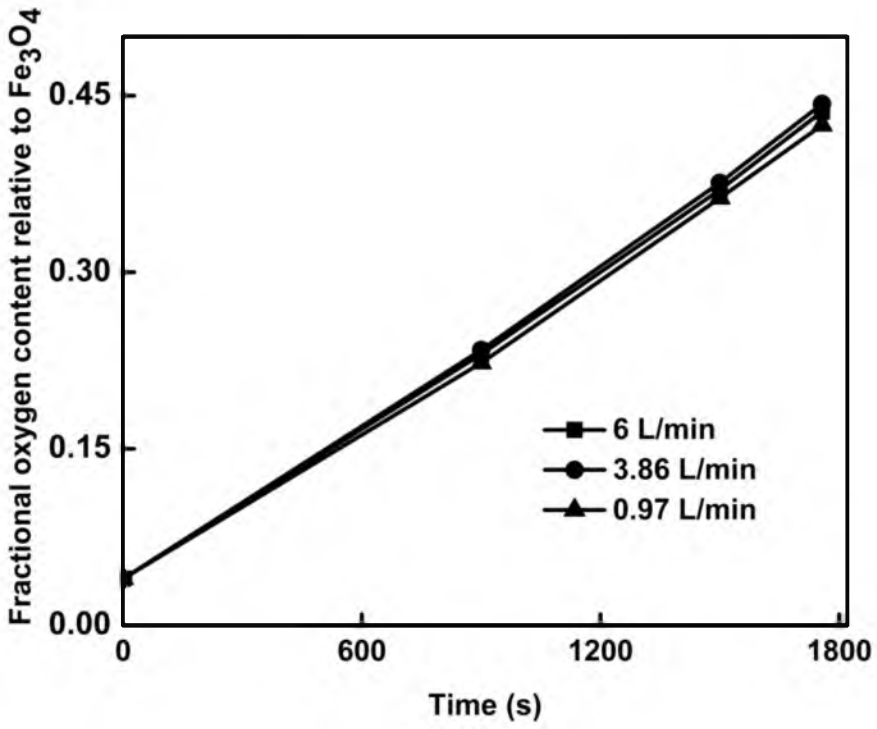

Fig. 10 Effect of gas flow rate on the reoxidation rate at 923 K (650 °C); p_{H_2O} / p_{H_2} = 80%/20%, P_{total} = 86.1 *kPa*

3.1.2 Reproducibility of Experimental Results

It is desirable to determine the reproducibility of the experimental results because solid particles usually have variations in morphology and crystal structure, thus causing scatter in experimental results.

Experiments at 873 K (600 °C) with 80 pct $H_2O(g)$ and constant sample sizes of 100 ± 5 mg were repeated several times at each duration of time and the results are shown in Figure 11 (P_{total} = 86.1 kPa). As can be seen, all the results were reproducible within ± 3 pct of the average value.

3.1.3 Effect on Reoxidation of the Reduction Temperature During the Preparation of Iron Particles

Iron particles with similar reduction degrees were produced at 1473 K (1200 °C) and 1623 K (1350 °C) in the flash reduction process.[27] Reoxidation experiments using these two types of iron particles were conducted at 973 K (700 °C) and the results in Figure 12 indicate that the reoxidation rates were close in both cases. This is explained by the similar microstructures of iron particles shown in Figure 13.

The proposed temperature range in the novel flash ironmaking process is 1500 – 1900 K, much higher than in the typical direct reduction processes.[11] Thus it is of interest to examine the differences of oxidation rates between the flash reduced iron particles and the conventional direct reduced iron particles. Fine magnetite concentrate was reduced by H_2 at 1073 K (800 °C) and by CO at 1223 K (950 °C) in a horizontal

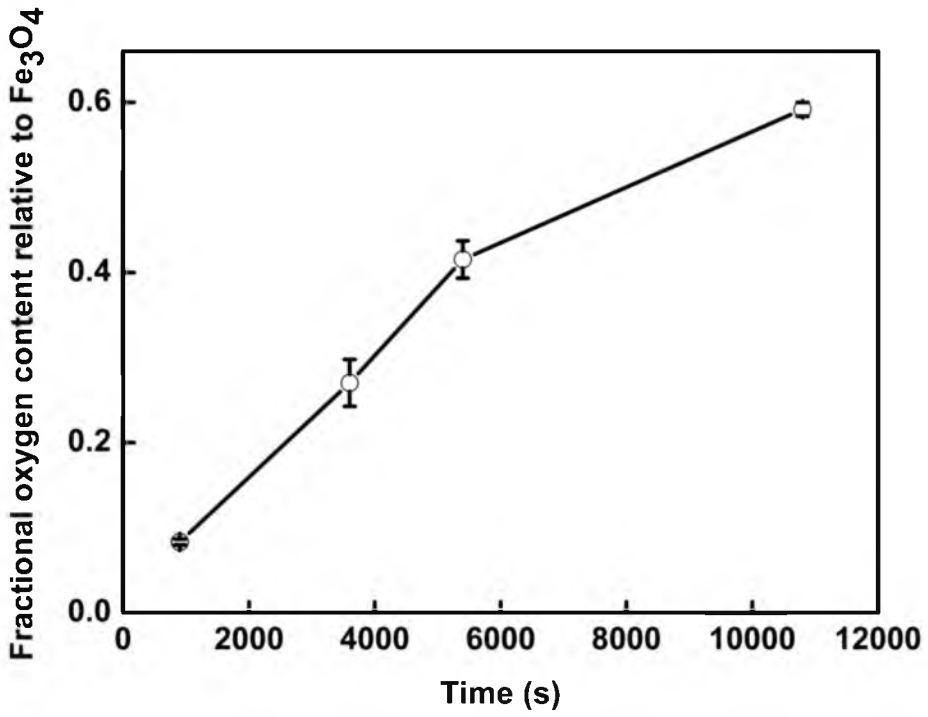

Fig. 11 Reproducibility test at 873 K (600 °C); p_{H_2O} / p_{H_2} = 80%/20%, P_{total} = 86.1 *kPa*

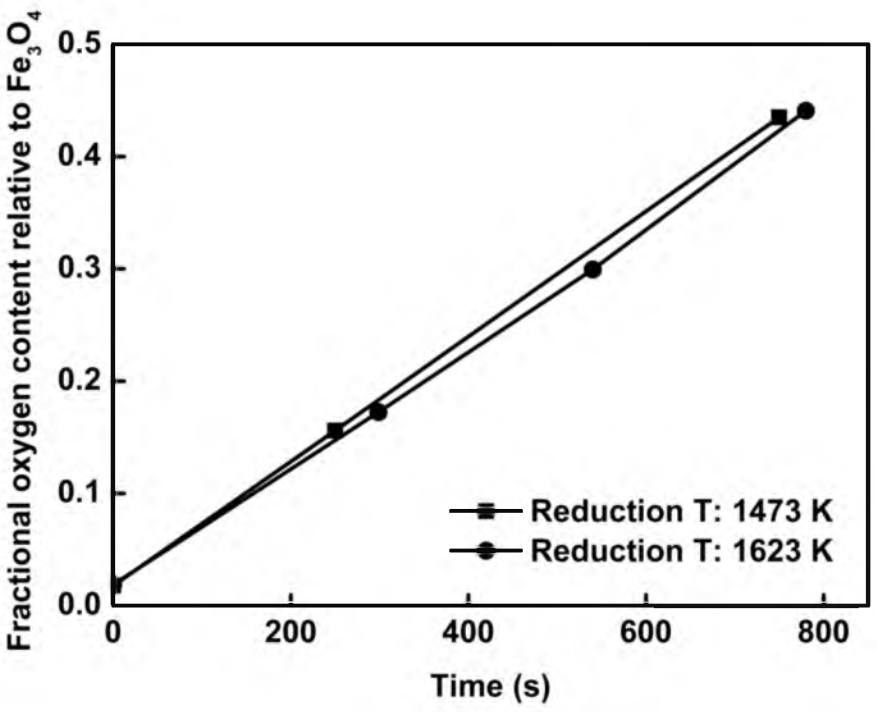

Fig. 12 Effect on the reoxidation rate of reduction temperature during the preparation of iron particles; 973 K (700 °C); p_{H_2O} / p_{H_2} = 80%/20%, P_{total} = 86.1 *kPa*

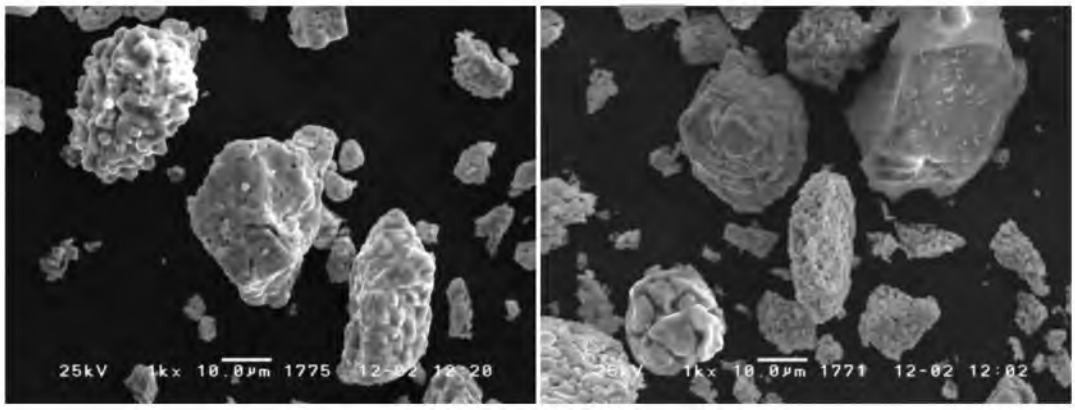

A) Reduction Degree: 96% at 1623 K B) Reduction Degree: 98% at 1473 K

Fig. 13 SEM micrographs of iron particles reduced at different temperatures

furnace to produce iron particles that are typical in conventional direction reduction processes. Reoxidation rates of these iron particles in H_2-H_2O were compared with that of the flash reduced iron particles produced at 1623 K (1350 °C). The results in Figure 14 and 15 show a slower oxidation rate for flash reduced iron particles. This is due to the lower specific surface area of iron particles produced at higher temperatures available in the novel flash ironmaking process. The data provided by the MICROMERITICS ASAP 2020 shows a specific surface area of 195 m^2/kg for flash reduced iron produced at 1623 K (1350 °C), whereas iron particles reduced by CO and H_2 at, respectively, 1223 K (950 °C) and 1073 K (800 °C) are, respectively, 228 and 457 m^2/kg. SEM pictures were taken for all three types of iron particles and in Figure 16 it can be clearly observed that iron particles produced at 1623 K (1350 °C) are more rounded, thus less reactive in oxidation.

3.1.4 Effects of H_2O Partial Pressure and Temperature

The influence of H_2O partial pressure on reoxidation was studied by varying the H_2O concentration from 40 to 100 pct in H_2O-H_2 mixtures (total pressure = atmospheric pressure in Salt Lake City = 86.1 *kPa*), while temperature and the total gas flow rate were, respectively, maintained at a fixed rate of 873 K (600 °C) and 6 L/min and other conditions were all kept identical. The results shown in Figure 17 indicate that the rate and degree of reoxidation increased with H_2O partial pressure as expected. The quantitative data will be used below to formulate the rate equation.

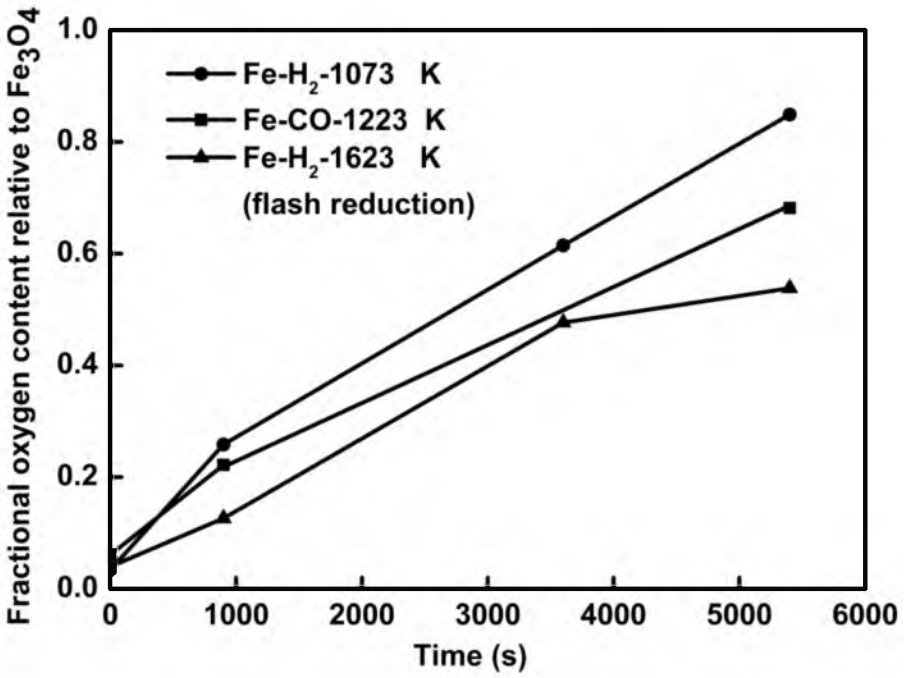

Fig. 14 Comparison of reoxidation rates of iron particles reduced at different temperatures; 873 K (600 °C), 100% H_2O, P_{total} = 86.1 *kPa*

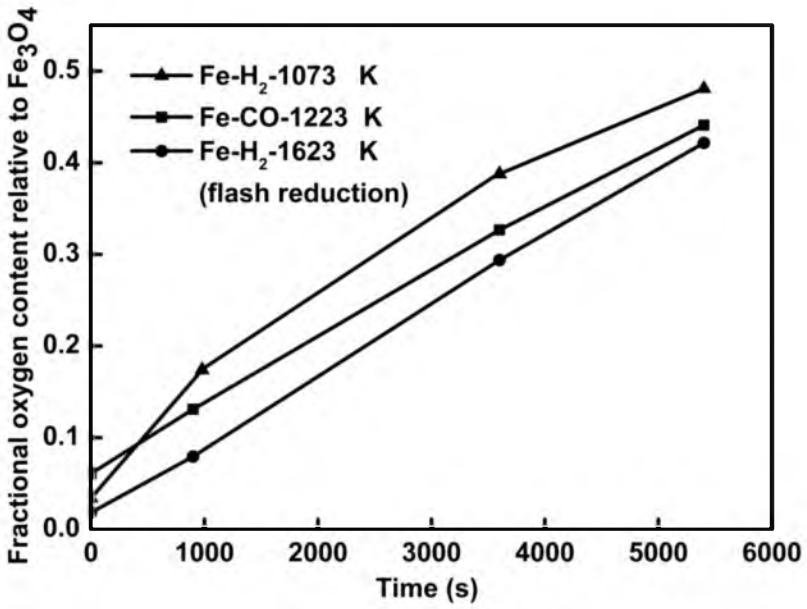

Fig. 15 Comparison of reoxidation rates of iron particles reduced at different temperature; 873 K (600 °C), p_{H_2O} / p_{H_2} = 60%/40%, P_{total} = 86.1 kPa

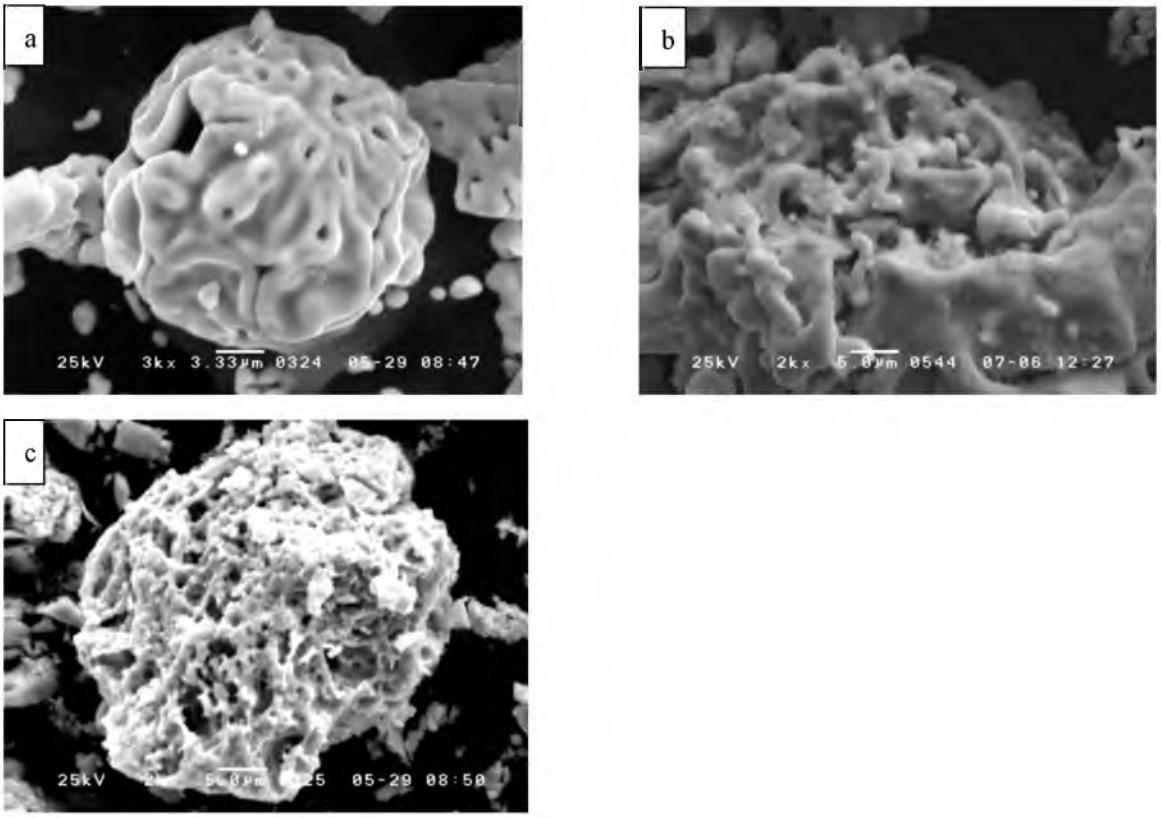

Fig. 16 Comparison of microstructures of different iron particles: a) flash reduced iron produced at 1623 K (1350 °C); b) CO reduced iron at 1223 K (950 °C); c) H_2 reduced iron at 1073 K (800 °C)

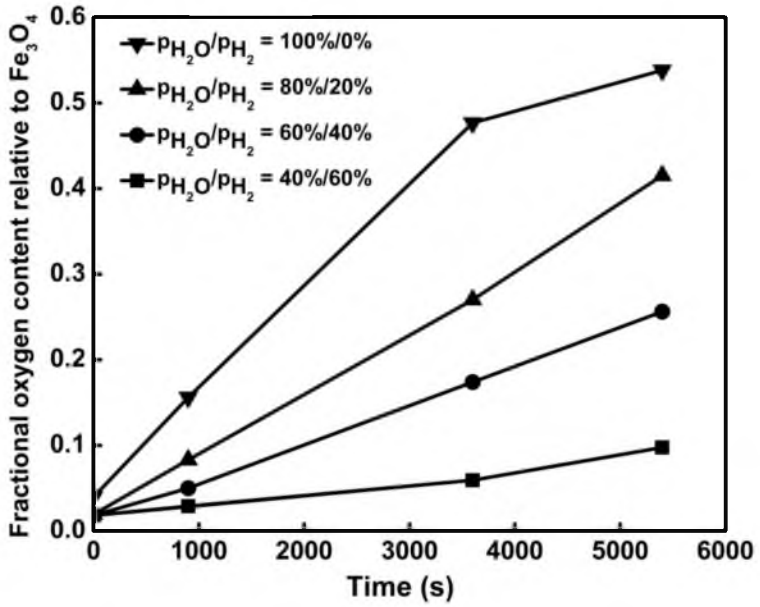

Fig. 17 Effect of H2O partial pressure on reoxidation rate at 873 K (600 °C); P_{total} = 86.1 *kPa* (the atmospheric pressure in Salt Lake City)

Temperatures were varied in the range of 823 - 973 K (550 - 700 °C) with the same $H_2O(g)$ concentrations of 80 pct and other identical conditions (P_{total} = 86.1 *kPa*). As expected, the rise in temperature resulted in faster reoxidation and a larger reoxidation degree, as indicated in Figure 18. Experiments were also conducted at even lower temperatures of 723 K (450 °C) and 773 K (500 °C). However, the reaction rates were too low to be measurable in the current system.

3.1.5 Reaction Mechanism and Rate Model

Gas solid reactions usually involve the adsorption of gaseous reactants at preferred sites on the solid surface and the formation of nuclei of the solid product. For small particles the period of the formation and growth of the nuclei occupies essentially the entire conversion range.[28] The nucleation and growth phenomenon in gas solid reactions are mentioned in many investigations.[29-31]

In the present study, scanning electron microscopy images of particles were taken at various stages of reoxidation. Figure 19 shows in the top two pictures the grains of the original iron particles and the very slightly oxidized ones are round because of the high reduction temperature used in the new process. In the bottom two pictures, after oxidation on the other hand, the grains are angular indicating oxide grains formed by the oxidation reaction.

Based on the observed evolution of nucleation and growth and the previous studies described above, the interpretation of the rate data was carried out using the nucleation

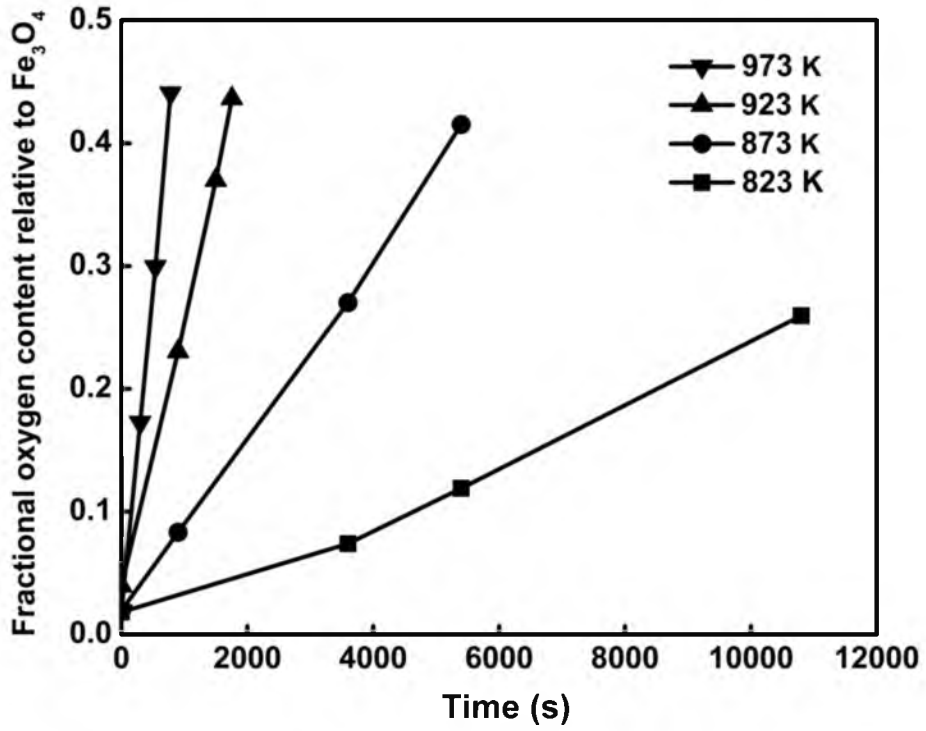

Fig. 18 Effect of temperature on reoxidation rate; p_{H_2O} / p_{H_2} = 80%/20%, P_{total} = 86.1 *kPa*

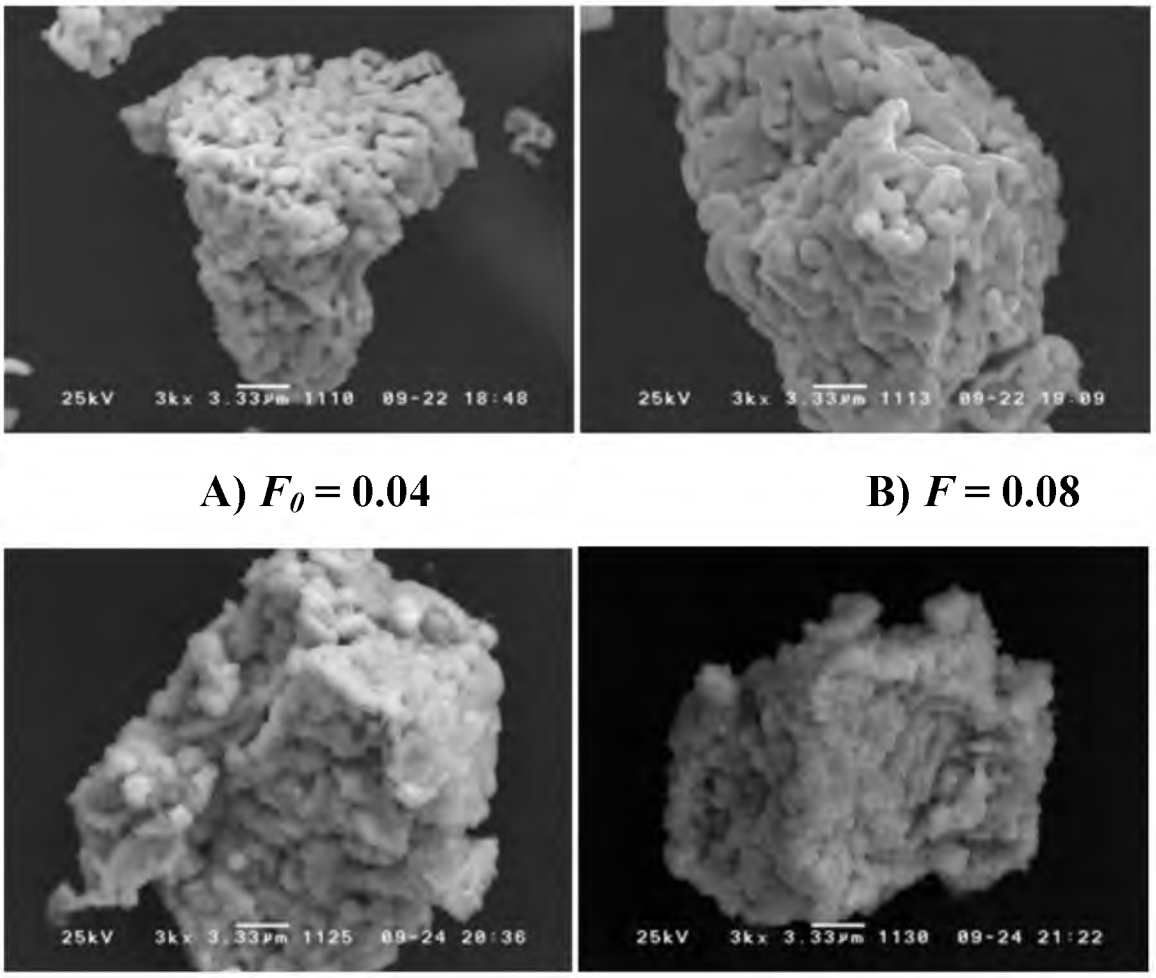

A) $F_0 = 0.04$ **B) $F = 0.08$**

C) $F = 0.42$ **D) $F = 0.59$**

Fig. 19 SEM micrographs of particles after reoxidation at 873 K (600 °C); p_{H_2O} / p_{H_2} = 80%/20%, P_{total} = 86.1 *kPa*

and growth kinetics. Indeed, the kinetics model was found to describe well the oxidation rate of iron particles. In this rate expression, the reoxidation degree of iron particles is related to the reaction time by[32]

$$\left[Ln\left(\frac{1-F_0}{1-F}\right)\right]^{1/m} = k_{app}\cdot t \qquad (19)$$

where m is the Avrami parameter, t the reaction time, F the fractional oxygen content relative to Fe_3O_4, F_0 the initial value of F at $t = 0$, k_{app} the apparent rate constant. m in the above equation is a geometric factor representing the dimensionality of nuclei growth, and therefore it is considered independent of temperature and gas partial pressure. According to the original theoretical derivation by Avrami,[33-35] the value of m is an integer between 1 and 4; however, m has been regarded as an adjustable parameter that could be a noninteger.[36] k_{app} is related to chemical reaction and varies with temperature and partial pressure, as expressed below,[23]

$$k_{app} = b\cdot k\cdot f_p\left(p_{H_2O}, p_{H_2}\right) \qquad (20)$$

where b is a stoichiometry coefficient (number of moles of solid reacted per mole of gaseous reactant = 1 in the present study), and k is the intrinsic rate constant, p_{H_2O} and p_{H_2} are, respectively, the partial pressures of H_2O and H_2, and f_p denotes the functional dependence on partial pressures. The validity of applying this model was examined by plotting $Ln\left[Ln\left(\frac{1-F_0}{1-F}\right)\right]$ versus $Ln\ t$. As seen in Figures 20 and 21, all data fit well as demonstrated by the straight lines with m = 1.26. This implies that the reoxidation kinetics obeys the rate equation and the Avrami parameter m is indeed independent of

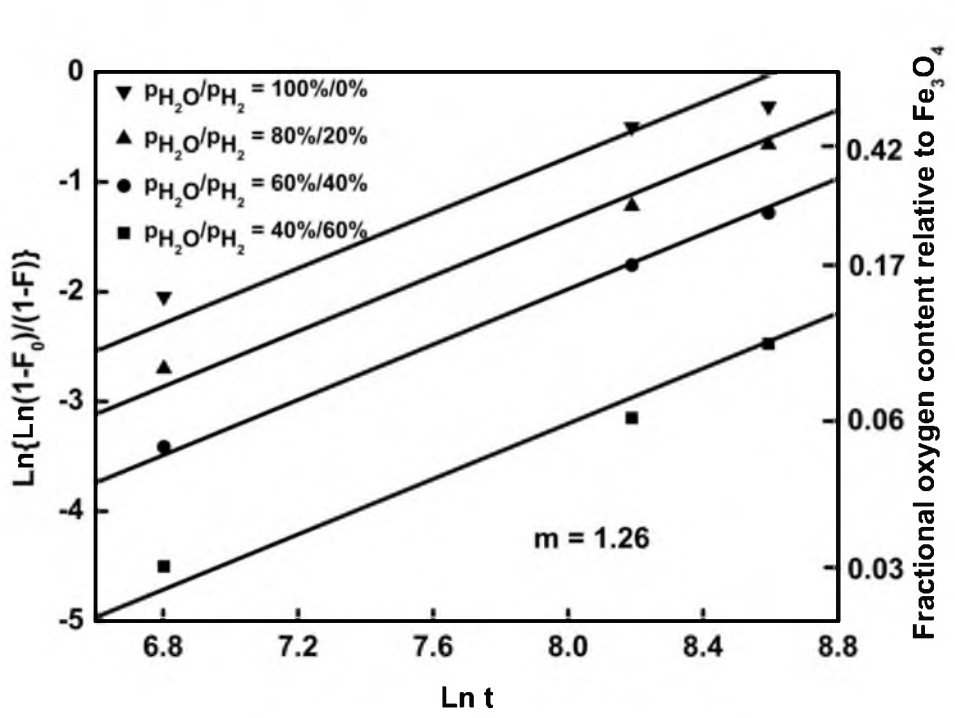

Fig. 20 Relationship between $Ln\left[Ln\left(\frac{1-F_0}{1-F}\right)\right]$ and *Ln t* at 873 K (600 °C); *m = 1.26*, P_{total} = 86.1 *kPa*

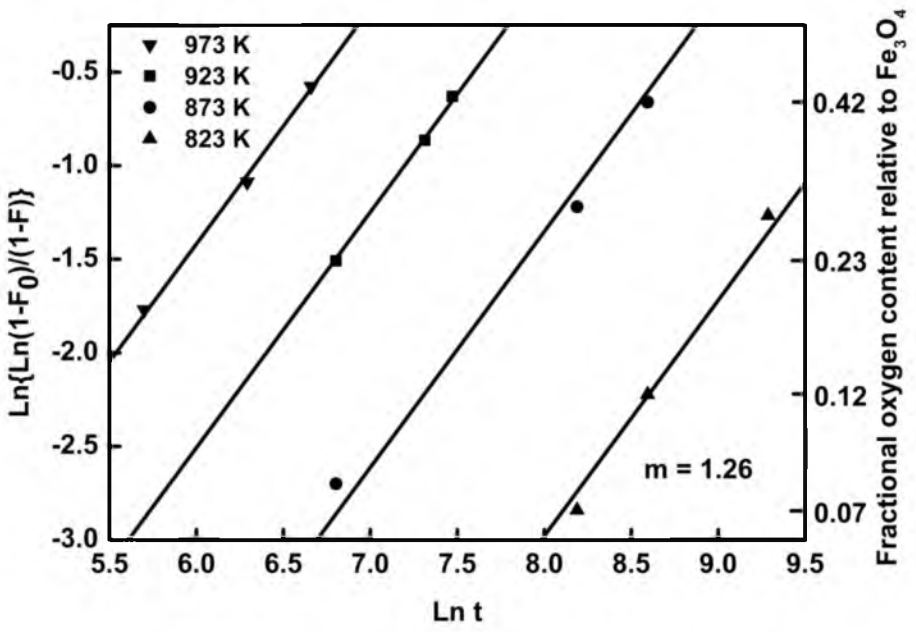

Fig. 21 Relationship between $Ln\left[Ln\left(\frac{1-F_0}{1-F}\right)\right]$ and $Ln\ t$ with p_{H_2O} / p_{H_2} = 80%/20%; m = *1.26*, P_{total} = 86.1 *kPa*

temperature and partial pressure. The reason that in the present study there was no detectable induction period at the beginning of the oxidation and no sigmoidal curves, as usually described by the nucleation and growth model, was because of the rapid nucleation rate and one dimensional nuclei growth in the temperature range of interest, as also mentioned by other investigations.[33,37,38]

In the work reported by Turkdogan *et al.*[12] and Yin *et al.*[13] on the oxidation of iron by H_2O gas, the oxidation of iron/steel strips was performed under a condition in which the oxide layer was very dense and covered the entire surface; so reaction proceeded through solid state diffusion after a brief initial period. In the oxidation of fine porous iron particles, the reaction proceeds through the formation and growth of individual nuclei of the oxide throughout the conversion range. There is thus a major difference in microstructures as far as the rate equation is concerned. Further, in the work of Turkdogan *et al.*[12] and Yin *et al.*[13] the surface area for reaction is quite well defined, whereas in the oxidation of fine porous iron particles the area for reaction is not only difficult to define but changes with the progress of reaction. Thus, in this case the change in reaction surface is included, albeit indirectly, in the term that contains fractional oxygen content. This is another major difference in the rate expressions.

Furthermore, the thickness of the dense oxide layers in the references mentioned above was much larger (30-400 microns) than the effective dimension of the iron phase in the iron particles used in this work (~ 1 micron as seen in Figure 19). Therefore, solid state diffusion controls the oxidation rate in the former, but the particles in this work

reacted through the formation and growth of iron oxide nuclei in the absence of or under much smaller effects of solid state diffusion. In other words, the very early stage of oxidation controlled by chemical reaction stated by Turkdogan *et al.*[12] persisted over the entire range of oxidation in the present work.

3.1.6 Determination of Reaction Order with Respect to H_2O Partial Pressure

The reaction rate is dependent on the partial pressures of both gases, since the reduction of wustite by hydrogen is significantly limited by equilibrium in the proposed temperature range of the flash ironmaking process. The rate dependence is expressed[23]

$$f_p\left(p_{H_2O}, p_{H_2}\right) = {p_{H_2O}}^n - \left(p_{H_2} / K\right)^n \qquad (21)$$

where K is the equilibrium constant of the oxidation of iron to wustite [or magnetite below 833 K (560 °C)] by $H_2O(g)$, and n is the reaction order with respect to H_2O and H_2 partial pressures. The last step of H_2 flash reduction of iron ore concentrate is significantly limited by equilibrium, therefore the reverse reaction, i.e., the oxidation of iron to wustite is likely to take place and the corresponding equilibrium constant should be used in Eq. (21). The above equation should satisfy the equilibrium condition, i.e., $K = p_{H_2} / p_{H_2O}$, at equilibrium and therefore the exponents on the two terms on the right hand of Eq. (21) should be the same.

In the study of hydrogen reduction kinetics of magnetite concentrate, Wang and Sohn[23] found a half order relationship best described the reaction rate. The first order relationship was also examined but found less satisfactory. Thus, in this research $n = 1$ (a

first order reaction) and n = 0.5 (a half order reaction) were both tested. The k_{app} values obtained from the plots of $Ln\left[Ln\left(\frac{1-F_0}{1-F}\right)\right]$ versus $Ln\ t$ are plotted against $p_{H_2O}{}^n - \left(p_{H_2} / K\right)^n$ according to Eq. (21). The result in Figure 22 indicates that n = 1 gives an excellent fit. However, within the concentration range tested, the fit for reaction order was indistinguishable in the range of 0.4 – 2, partly because of the significant value of the second term. From the reaction mechanism point of view, however, the reaction needs adsorption of one H_2O molecule to produce the one atom of oxygen that is needed to produce wustite. Thus it appears most appropriate to select first order with respect to H_2O partial pressure. A first order dependence was also observed by Smeltzer[39] for iron oxidation in CO_2-CO gas mixtures. For iron oxidation in O_2, on the other hand, Pfeiffer and Laubmeyer[40] determined a partial pressure dependence of 0.7.

3.1.7 Determination of Activation Energy

With the partial pressure dependence determined, the reaction rate constant k can be obtained by rearranging Eq. (20). The activation energy was determined by the slope of the plot of *Ln k* versus *1/T,* shown in Figure 23.

$$k = k_{app} / f_p\left(p_{H_2O}, p_{H_2}\right) = k_{app} / \left[p_{H_2O} - \left(p_{H_2} / K\right)\right] \tag{22}$$

$$k = A \cdot exp\left(-E / RT\right) \tag{23}$$

$$Lnk = LnA - \frac{E}{R} \cdot \frac{1}{T} \tag{24}$$

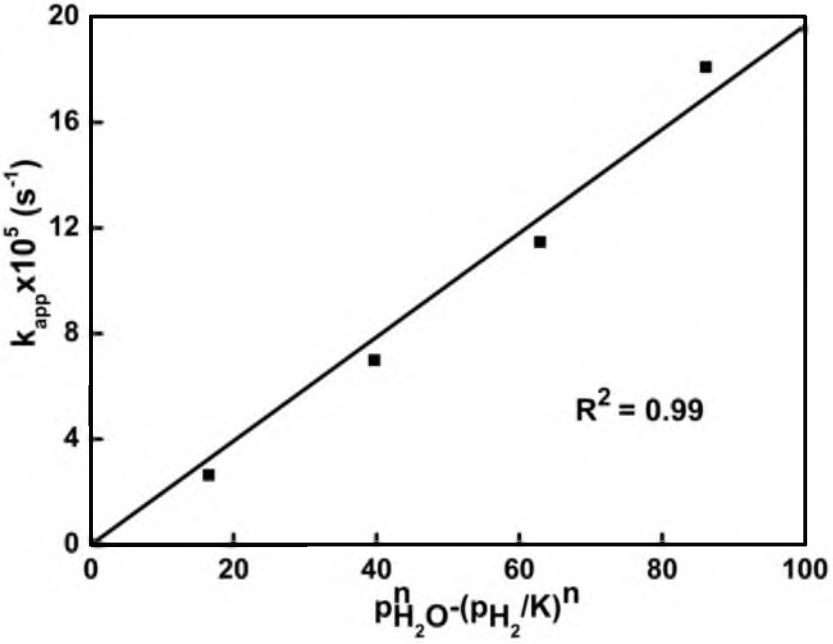

Fig. 22 Relationship between k_{app} and $p_{H_2O}{}^n - \left(p_{H_2} / K\right)^n$, $n = 1$, p in kPa

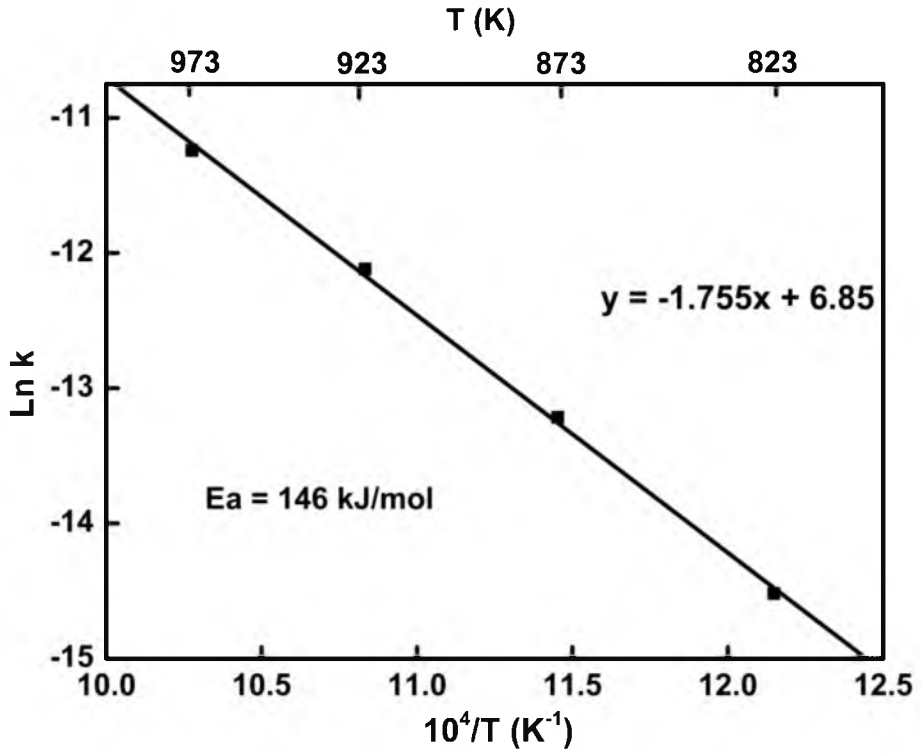

Fig. 23 Arrhenius plot between *Ln k* and $10^4/T$; *k* in $s^{-1} \cdot kPa^{-1}$

The slope of the straight line corresponded to an activation energy of 146 kJ/mol. The complete expression for the rate constant k is then given as

$$k = 941.5 \cdot exp\left(-146000 / RT\right) s^{-1} \cdot kPa^{-1} \qquad (25)$$

3.1.8 Complete Rate Equation

At a constant temperature, the relationship between the fractional oxygen content relative to Fe_3O_4 (F) and time is given below by combining Eqs.(19) – (21) and (25):

$$\left[Ln\left(\frac{1-F_0}{1-F}\right)\right]^{1/1.26} = 941.5 \cdot exp\left(-\frac{146000}{RT}\right) \cdot \left(p_{H_2O} - p_{H_2} / K\right) \cdot t \qquad (26)$$

where F_0 is the initial fractional oxygen content relative to Fe_3O_4, K is the equilibrium constant of oxidation of iron to wustite [or magnetite below 833 K (560 °C)] by $H_2O(g)$, T is in K, p is in *kPa,* and t is in second.

The instantaneous rate of reoxidation can thus be obtained as

$$\frac{dF}{dt} = 1.26 \cdot k \cdot \left(p_{H_2O} - p_{H_2} / K\right) \cdot \left(1-F\right) \cdot \left[Ln\left(\frac{1-F_0}{1-F}\right)\right]^{1/4.85} \qquad (27)$$

where $k = 941.5 \cdot exp\left(-146000 / RT\right)$

The rate equation applies to iron particles produced from Fe_3O_4 in the temperature range of 1473 – 1673 K (1200 – 1400 °C).

Comparisons are made between the experimental data and the results calculated from the rate equation. As can be seen in Figures 24, 25 and 26, the calculated results agree well with the experimental data.

The main purpose of this research was to obtain a complete rate equation that

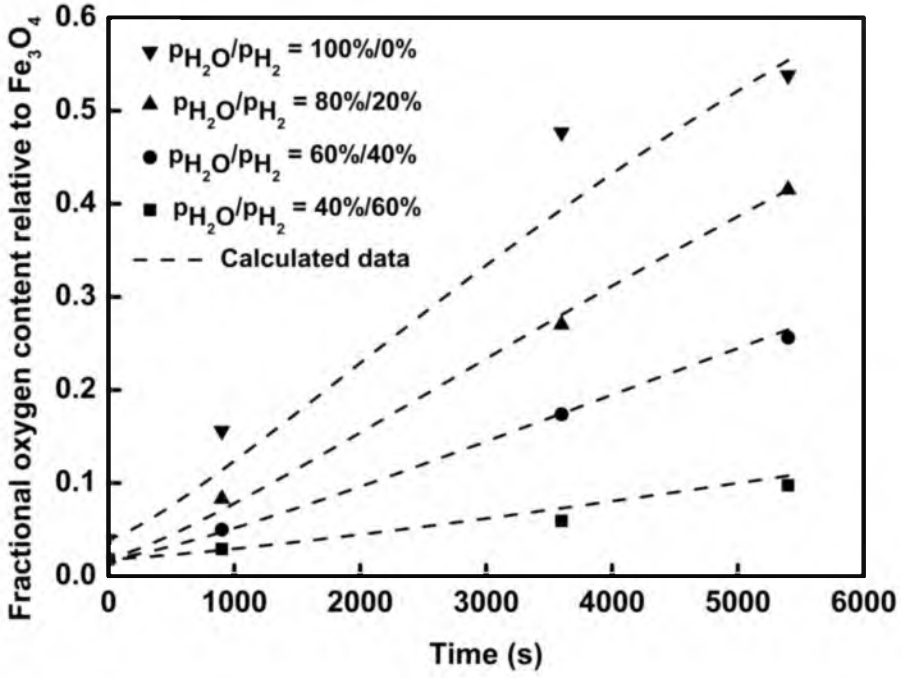

Fig. 24 Comparison between the calculated F versus time and experimental F versus time, 873 K (600 °C), P_{total} = 86.1 kPa

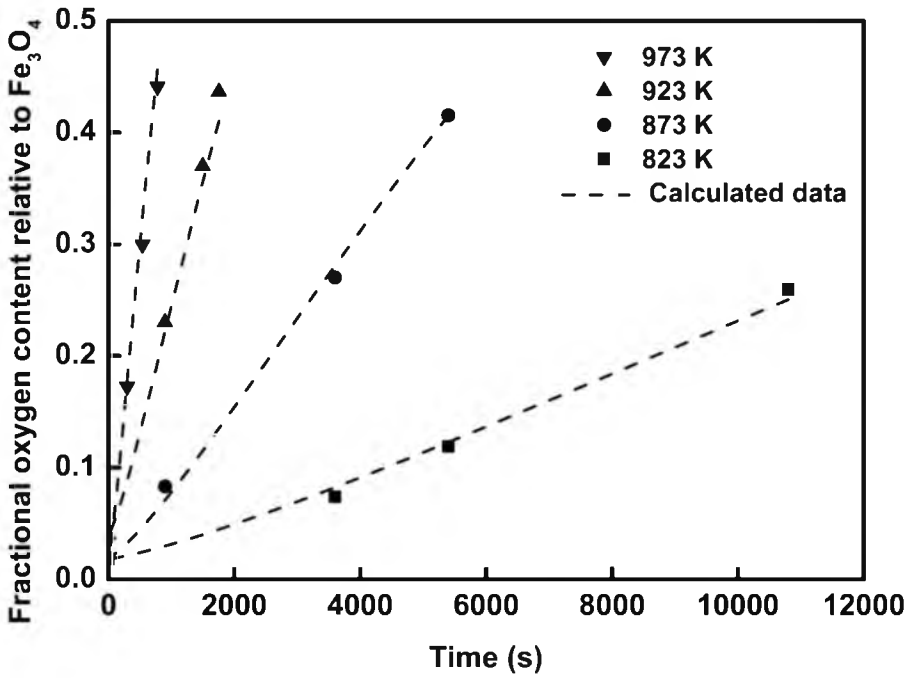

Fig. 25 Comparison between the calculated F versus time and experimental F versus time, p_{H_2O} / p_{H_2} = 80%/20%, P_{total} = 86.1 kPa

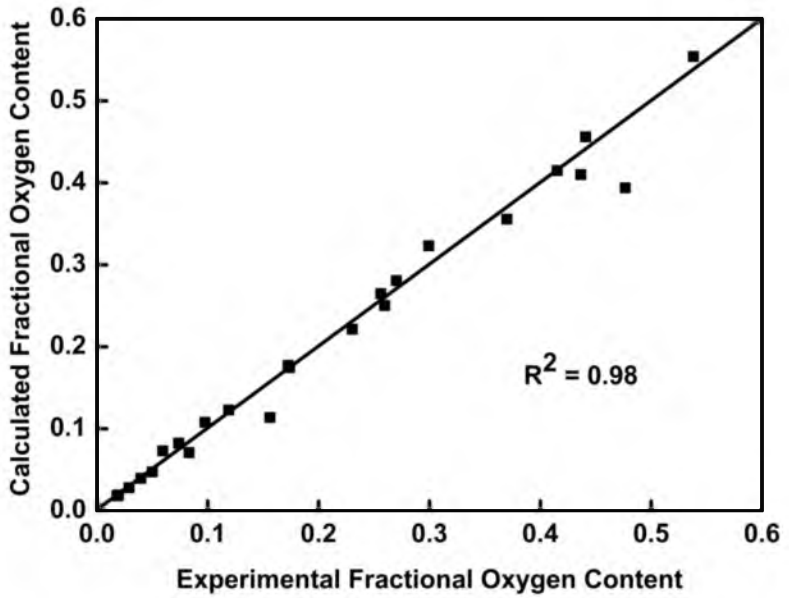

Fig. 26 Comparison between the calculated and experimental results in H_2-H_2O

predicts the loss of metallic iron through reoxidation in H_2-H_2O mixtures in the novel flash ironmaking process. Thus, it is of greater interest to study the reoxidation rate at low extents than to obtain the entire conversion range. In this regard, the rate equation provides satisfactory prediction of iron loss up to moderate reoxidation extents.

3.2 Reoxidation in O_2-N_2 Gas Mixtures

3.2.1 Elimination of Mass Transfer Effects

In order to eliminate the external mass transfer effect of reactant gas molecules, different flow rates of gas mixture were tested at 973 K (700 °C) on the iron particles reduced by H_2 at 1073 K (800 °C) with a fixed sample size of 120 ± 3 mg. This type of iron particle was selected because it has the highest specific surface area, 457 m^2/kg, compared with other types of iron particles used in research, i.e., iron particles reduced by CO at 1223 K (950 °C), 228 m^2/kg, and flash reduced iron by H_2 at 1623 K (1350 °C), 195 m^2/kg and thus the most reactive. Therefore, if mass transfer effect is removed for this sample, experiments with other less reactive iron particles are free from mass transfer effect. As seen in Figure 27, the reaction rate remained independent of gas flow rate above 1.36 NL/min. Plus, the highest gas mixture flow rate, 1.75 NL/min, was used in the subsequent runs to ensure the complete removal of external mass transfer effect.

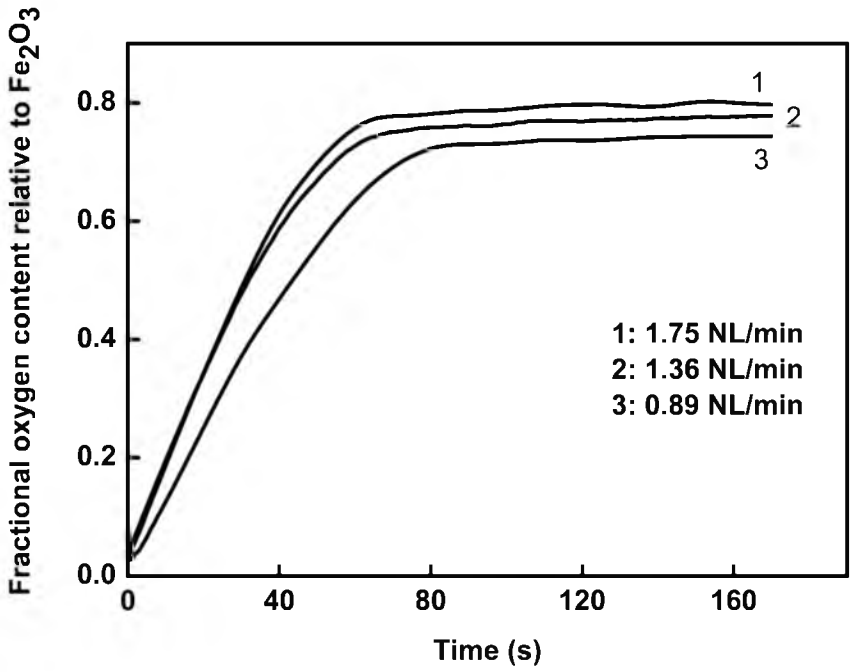

Fig. 27 Effect of gas flow rate on the reoxidation rate at 973 K (700 °C); p_{O_2} / p_{N_2} = 21%/79%, P_{total} = 86.1 kPa

3.2.2 Effects on Reoxidation of the Reduction Temperature During the Preparation of Iron Particles

Oxidation rate of iron particles [flash reduced by H_2 at 1623 K (1350 °C)] at 873 K (600 °C) with p_{O_2} / p_{N_2} = 21%/79% (P_{total} = 86.1 *kPa*) was compared with iron particle reduced by H_2 at 1073 K (800 °C), which is typical in conventional direct reduction ironmaking process. It is clear in Figure 28 that flash reduced iron particles are much more resistant to oxidation, due to a lower specific surface area (195 versus 457 m^2/kg).

3.2.3 Effects of O_2 Partial Pressure and Temperature

Different O_2 concentrations were used in the mixture of N_2 and O_2 to study the dependence of reoxidation rate on O_2 partial pressure. As O_2 concentration decreased from 21% to 5% at 873 K (600 °C), the reoxidation rate became much slower, as shown in Figure 29 (P_{total} = 86.1 *kPa*). The quantitative data will be used to determine the dependence of oxidation rate on oxygen partial pressure.

Reoxidation of flash reduced iron was conducted as temperature varied in the range of 673 - 873 K (400 – 600 °C) with gas mixture flow rate of 1.75 NL/min. Figure 30 shows that the reaction rates are much faster than those in water vapor and quickly level off at a low degree. Experiments were also conducted at lower temperatures such as 473 K (200 °C) and 573 K (300 °C), however, the reaction rate was too slow to be measured in the available TGA system. This also implies that the iron particles produced in the novel flash ironmaking process are resistant to oxidation at moderately low temperatures,

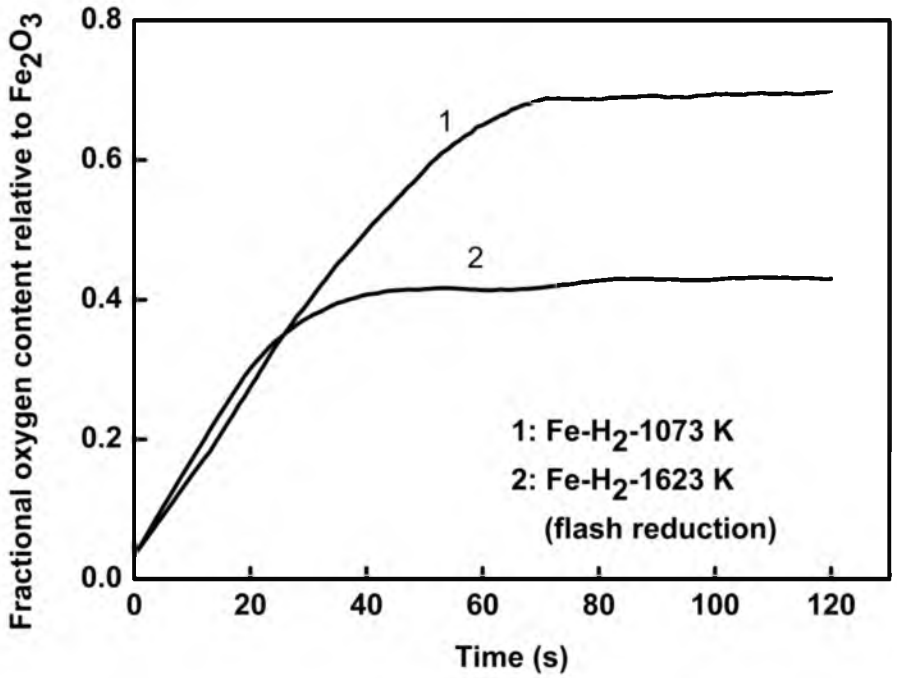

Fig. 28 Comparison of reoxidation rates of iron particles reduced at different temperatures; 873 K (600 °C), p_{O_2} / p_{N_2} = 21%/79%, P_{total} = 86.1 kPa

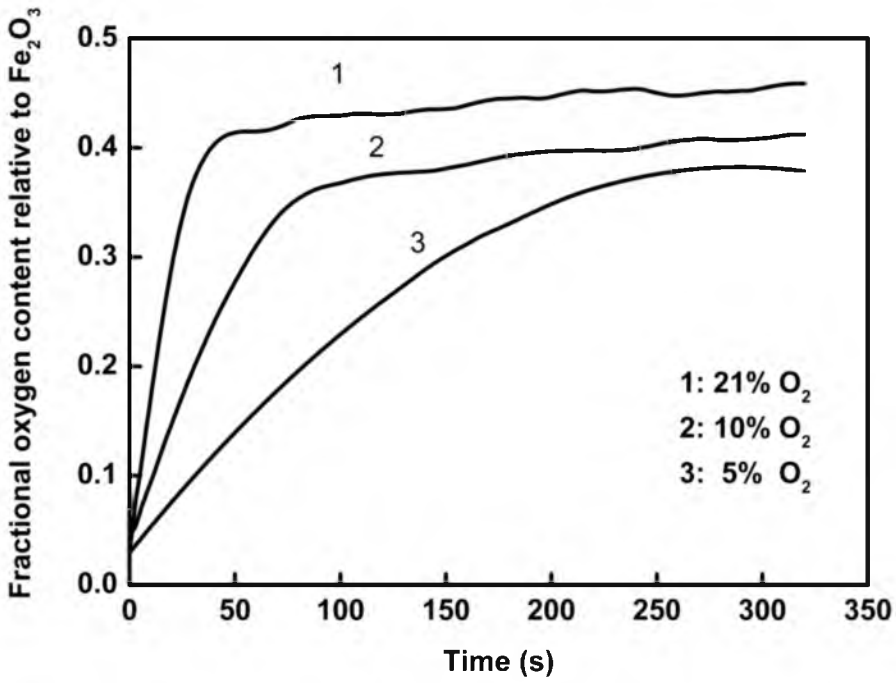

Fig. 29 Effect of O_2 partial pressure on reoxidation rate at 873 K (600 °C); P_{total} = 86.1 *kPa* (the atmospheric pressure in Salt Lake City)

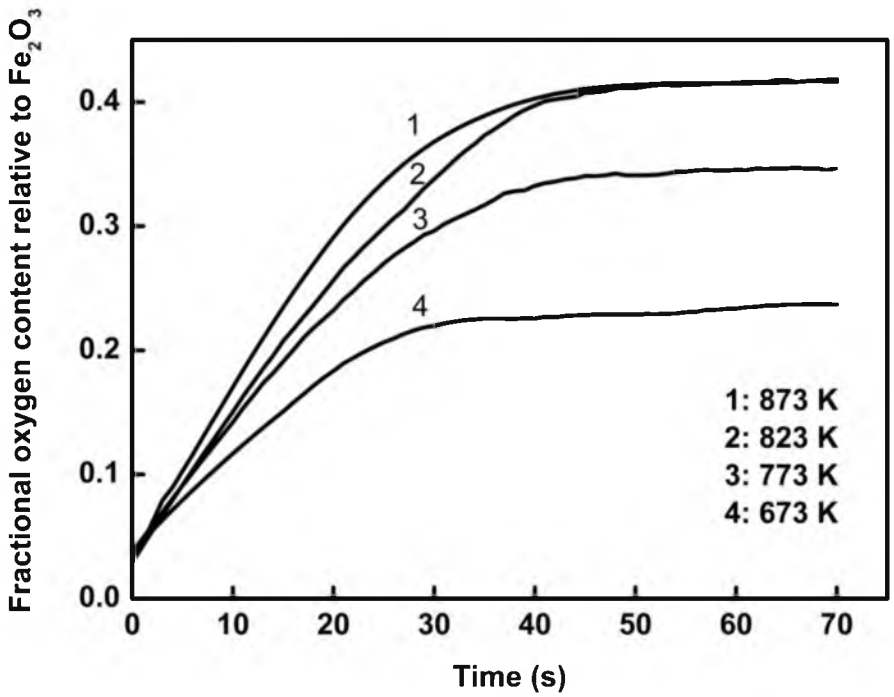

Fig. 30 Effect of temperature on reoxidation rate; p_{O_2} / p_{N_2} = 21%/79%, P_{total} = 86.1 *kPa*

due to low specific surface area.

3.2.4 Reaction Mechanism and Rate Model

SEM pictures in Figure 31 show the microstructures of starting iron particles and oxygen oxidized samples. From the comparison, it can be clearly seen that the oxide grains develop on the iron particles after oxidation. It was also reported[41] that the oxidation of iron in oxygen starts as nucleation of iron oxides occurs on the surface of iron. Therefore, the nucleation and growth model expressed in Eq. (19) was again employed to fit the oxidation data till the level off point. Figures 32 and 33 show that all data can fit very well with m = 1. The Avrami parameter m is again independent of temperature and pressure and m = 1 implies one dimensional oxide nuclei growth and explains the absence of a detectable induction period at the beginning of oxidation[33,37,38].

At the last stage, the rate becomes almost flat, probably due to the formation of a dense nonporous oxide layer causing a very slow diffusion of oxygen. A closer look at the microstructure of oxidized iron particles reveals the dense oxide layer on the surface in Figure 34. Oxidation of iron in oxygen is strongly exothermic compared with water vapor and carbon dioxide, as for example at 873 K (600 °C) in Eqs. (28), (29), (30). Therefore, it is believed that the strong reaction heat results in local fusion, causing the rounding of surface morphology and impeding the diffusion of reactant oxygen.

$$4/3\ Fe + O_2 = 2/3\ Fe_2O_3 \quad \Delta H = -539\ kJ/mol \tag{28}$$

$$Fe + H_2O = FeO + H_2 \quad \Delta H = -17\ kJ/mol \tag{29}$$

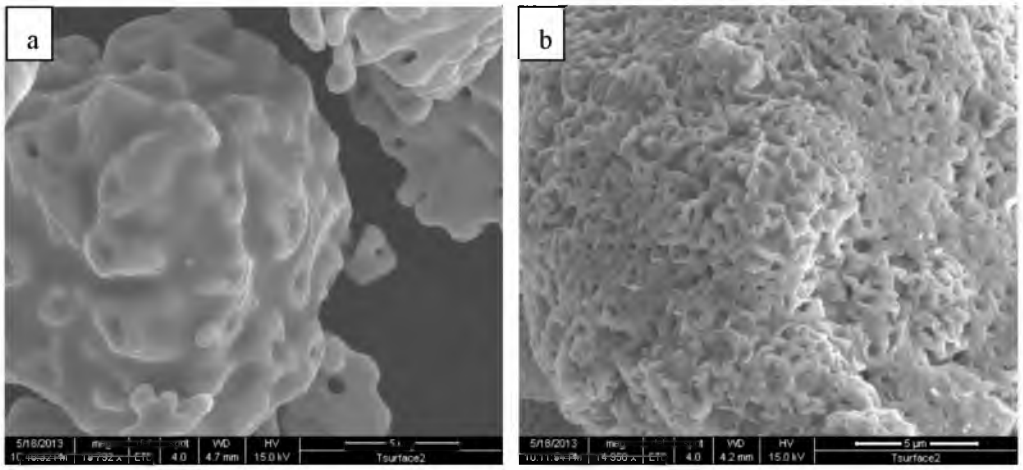

Fig. 31 SEM micrographs of a) starting iron particle; b) oxidized iron, $F = 0.47$ at 873 K

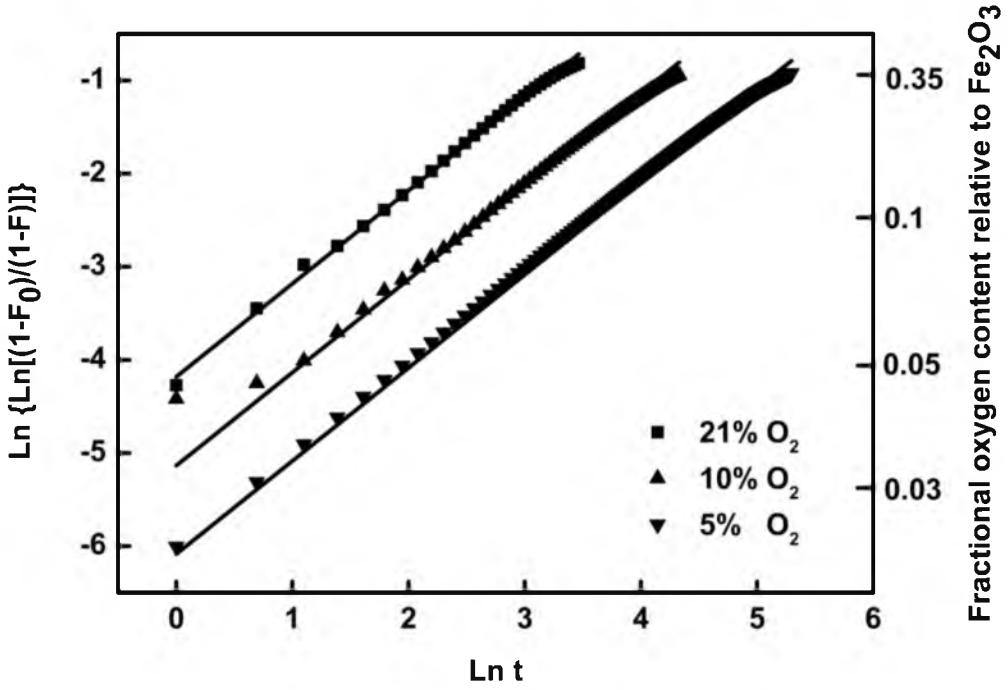

Fig. 32 Relationship between $Ln\left[Ln\left(\frac{1-F_0}{1-F}\right)\right]$ and $Ln\ t$ at 873 K (600 °C); $m = 1$, P_{total} = 86.1 kPa

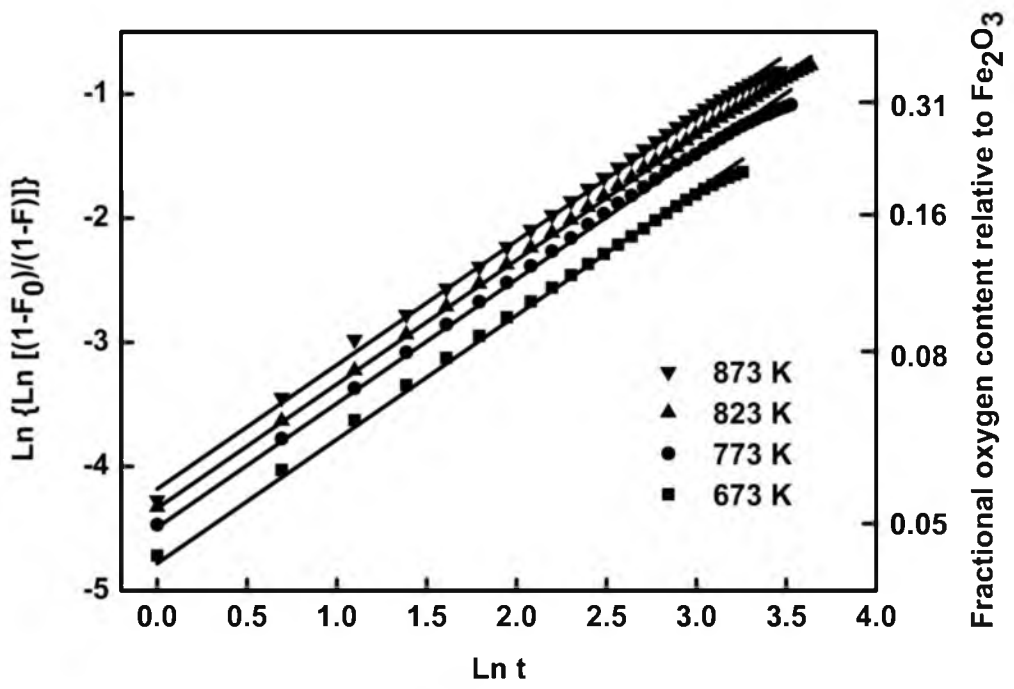

Fig. 33 Relationship between $Ln\left[Ln\left(\frac{1-F_0}{1-F}\right)\right]$ and $Ln\ t$ with p_{O_2} / p_{N_2} = 21%/79%; m = *1*, P_{total} = 86.1 kPa

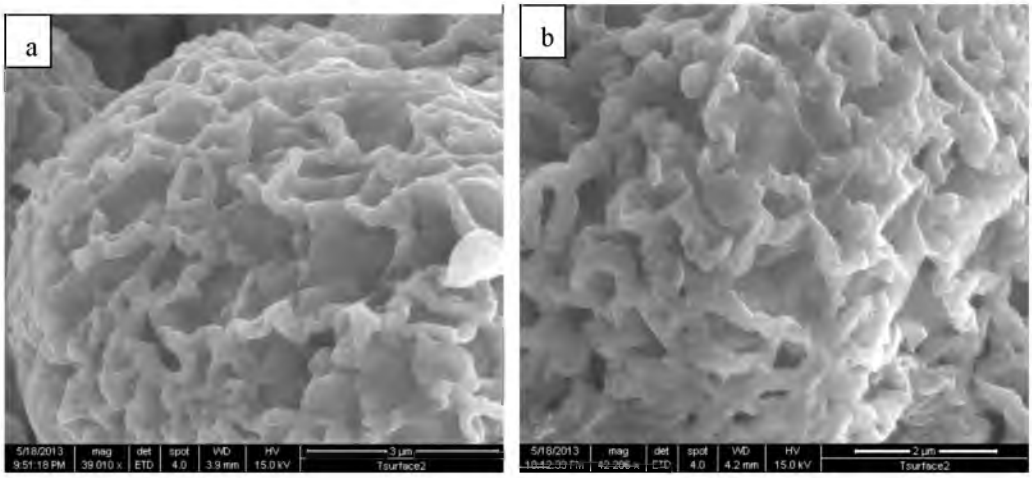

Fig. 34 SEM micrographs of a) oxidized iron, F = 0.36 at 873 K (600 °C); b) oxidized iron, F = 0.47 at 873 K (600 °C)

$$Fe + CO_2 = FeO + CO \quad \Delta H = 19 \text{ kJ/mol} \tag{30}$$

3.2.5 Determination of Reaction Order with Respect to Oxygen Partial Pressure

The reaction in consideration is

$$4/3 \ \ Fe + O_2 = \ \ 2/3 \ \ Fe_2O_3 \tag{31}$$

The apparent rate constant in Eq. (19) is related to the oxygen partial pressure as[42]

$$k_{app} = b \cdot k \cdot f_p\left(p_{O_2}\right) = b \cdot k \cdot p_{O_2}{}^n \tag{32}$$

where b is stoichiometry coefficient (number of moles of solid reacted per mole of gaseous reactant = 4/3 for iron oxidation in O_2), k the intrinsic rate constant, n the reaction order with respect to oxygen partial pressure, p_{O_2} partial pressure in kPa. k_{app} values from Figure 32 were plotted against $p_{O_2}{}^n$. Various values of n were tested and a first order relationship was found to be the most satisfactory as shown in Figure 35.

3.2.6 Determination of Activation Energy

From Eq. (32) the intrinsic rate constant k is expressed as

$$k = 3/4 \cdot k_{app} / p_{O_2} \tag{33}$$

The activation energy of the reoxidation reaction was obtained through the Arrhenius equation as 14.4 kJ/mol in Figure 36. The rate constant k is expressed as

$$k = 0.0045 \cdot exp\left(-\frac{14400}{RT}\right) s^{-1} \cdot kPa^{-1} \tag{34}$$

where T is temperature in K, and R is the gas constant.

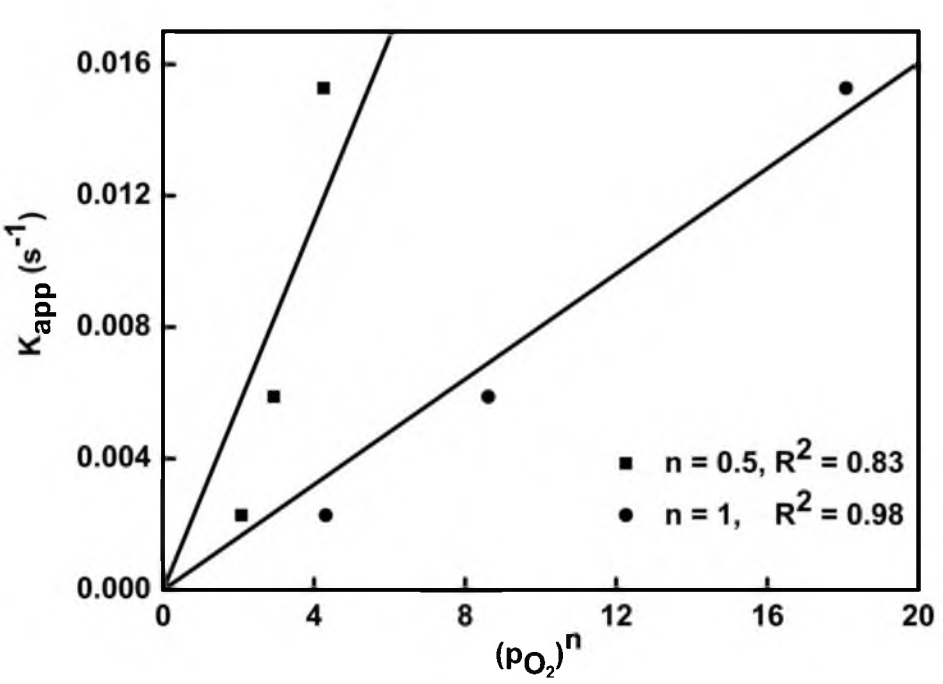

Fig. 35 Relationship between k_{app} and $p_{O_2}{}^n$, $n = 0.5$ and $n = 1$, p in kPa

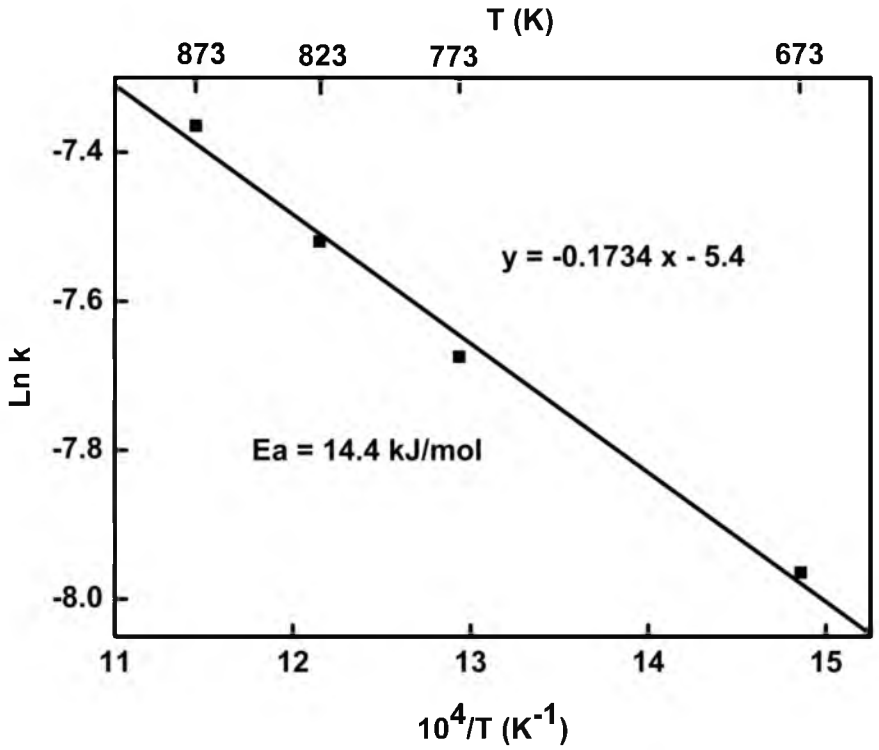

Fig. 36 Arrhenius plot between $Ln\ k$ and $10^4/T$; k in $s^{-1} \cdot kPa^{-1}$

3.2.7 Complete Rate Equation

For the reoxidation, until the level off point, the relationship between the fractional oxygen content and the time is formulated by combining Eqs. (19), (32), (34) as,

$$Ln\left(\frac{1-F_0}{1-F}\right) = 0.006 \cdot exp\left(-\frac{14400}{RT}\right) \cdot p_{O_2} \cdot t \qquad (35)$$

where F is the fractional oxygen content relative to Fe_2O_3, p_{O_2} is partial pressure of oxygen in *kPa*, and t is time in second

After the leveling off point, the rate can be regarded as constant based on Figure 29 and 30, and thus the F values of leveling off is related to temperature in Figure 37 as,

$$F = -3.05 \times 10^{-6} T^2 + 5.7 \times 10^{-3} T - 2.23 \qquad (36)$$

Therefore, the complete rate equation for reoxidation of flash reduced iron in O_2-N_2 is

$$Ln\left(\frac{1-F_0}{1-F}\right) = 0.006 \cdot exp\left(-\frac{14400}{RT}\right) \cdot p_{O_2} \cdot t, F < F_{level\text{-}off}$$

$$F_{level\text{-}off} = -3.05 \times 10^{-6} T^2 + 5.7 \times 10^{-3} T - 2.23, T > 573 \text{ K} \qquad (37)$$

and comparisons are made between the calculated F values from Eq. (37) and the experimental F. Rather good correlations are seen from Figure 38 for oxidation at different temperatures with p_{O_2} / p_{N_2} = 21%/79% (P_{total} = 86.1 *kPa*). For oxidation with lower oxygen concentrations, however, the correlation is not very satisfactory (Figure 39). As far as an ironmaking process is concerned, oxidation of iron particles in air during transportation is the major concern, and thus the oxidation can be predicted reasonably well by the rate equation.

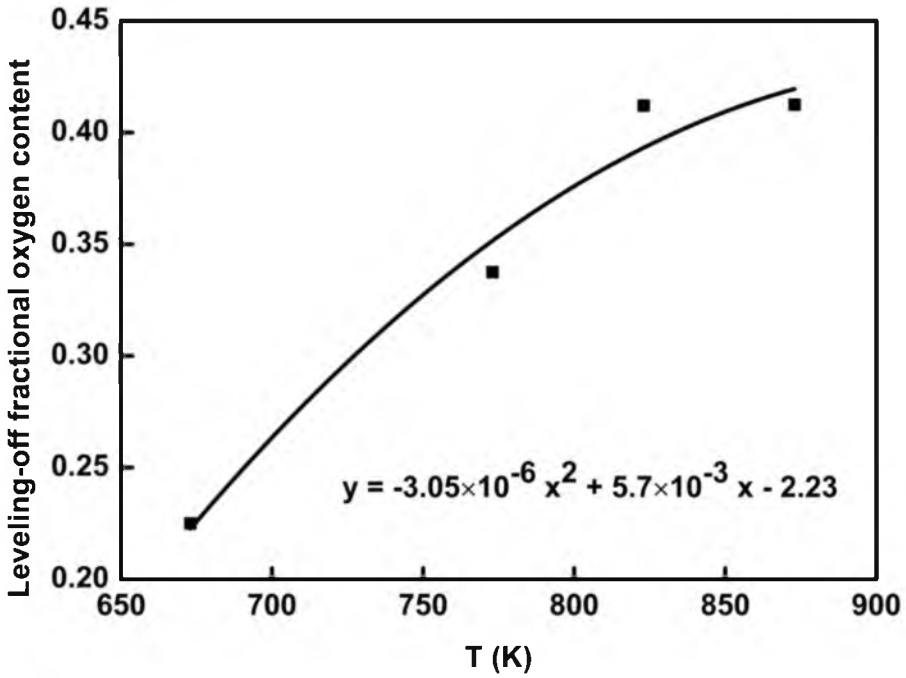

Fig. 37 Relationship between leveling off F and temperature

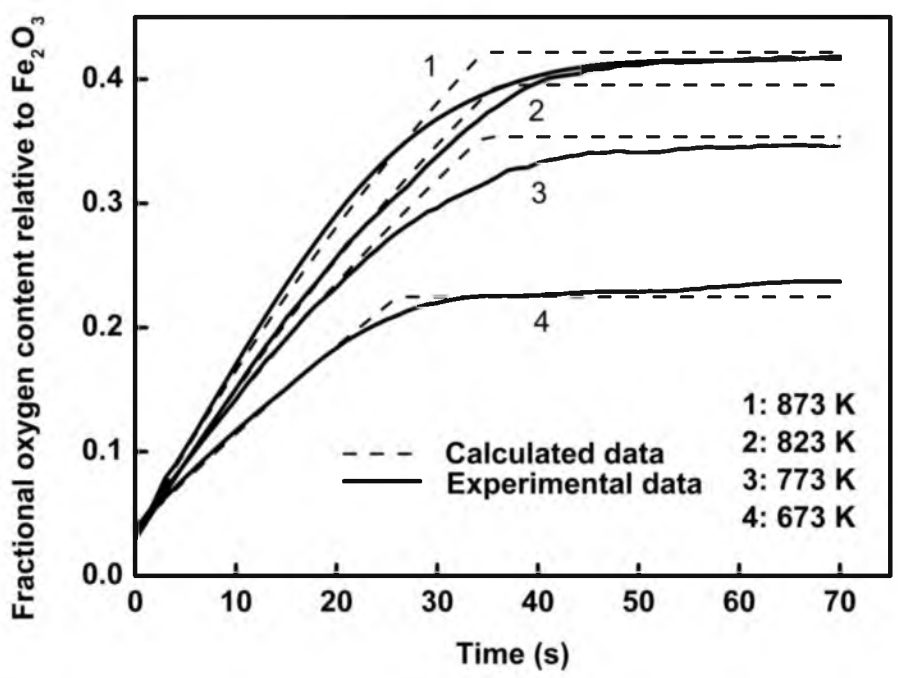

Fig. 38 Comparison between the calculated F versus time and experimental F versus time, p_{O_2} / p_{N_2} = 21%/79%, P_{total} = 86.1 kPa

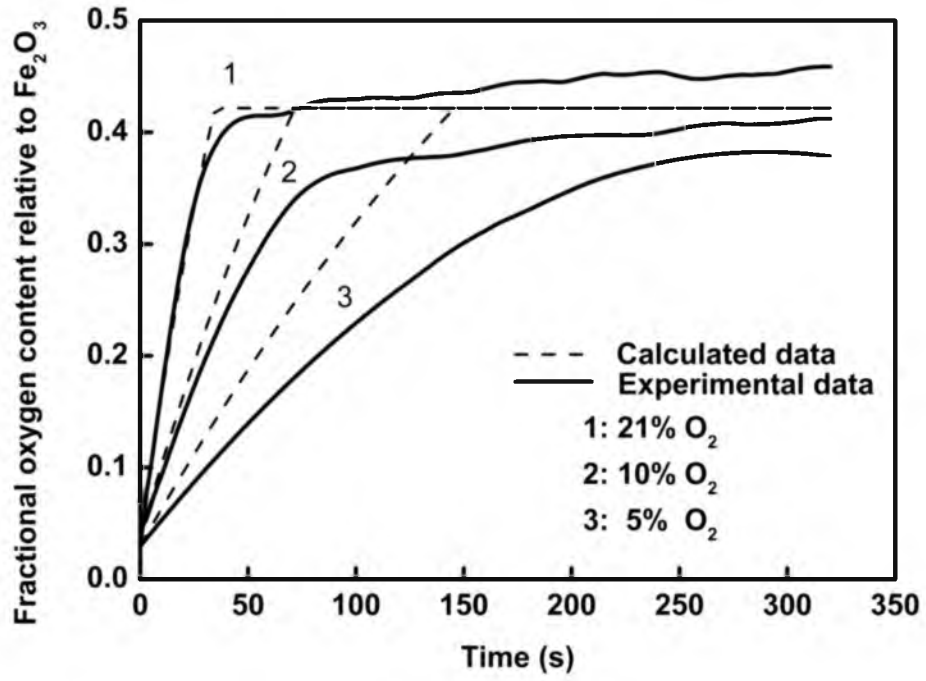

Fig. 39 Comparison between the calculated F versus time and experimental F versus time, 873 K (600 °C), P_{total} = 86.1 kPa

3.3 Reoxidation in CO_2

3.3.1 Effect of Temperature

The reoxidation of flash reduced iron in pure CO_2 was carried out in the temperature range of 873 – 1073 K (600 – 800 °C). Microstructures of oxidized particles in Figure 40 clearly show that crystallites of iron oxides form on the surface after oxidation. The kinetics results in the Figure 41 show that the oxidation in CO_2 is much slower than that in water vapor or oxygen. In addition, it can be concluded that both in the suspension reduction process, where the residence time of iron particles is typically less than 10 seconds, and in the collection bin, where the iron product may be kept for up to one hour at around 573 K (300 °C), the oxidation by CO_2 is not of concern due to its slow reaction kinetics.

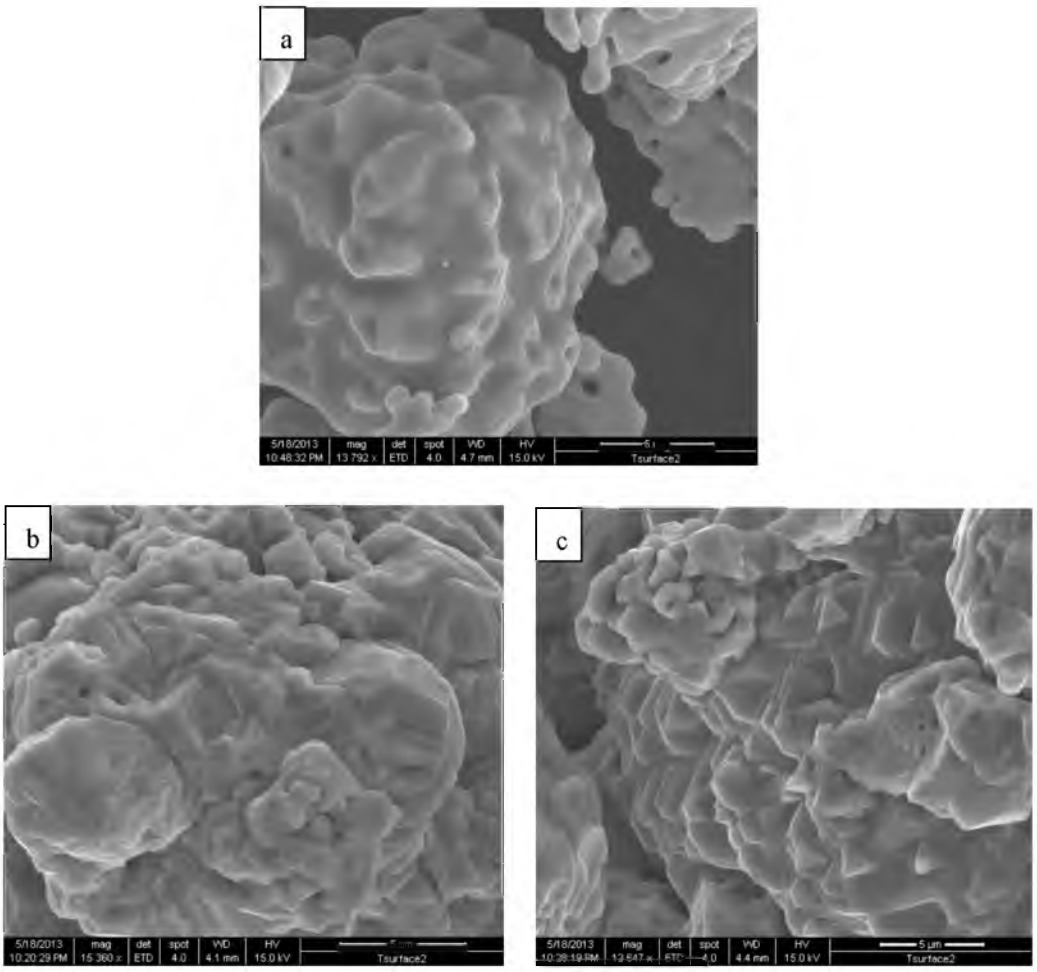

Fig. 40 SEM micrographs of a) starting iron particle; b) oxidized iron, F = 0.6; c) oxidized iron, F = 0.97

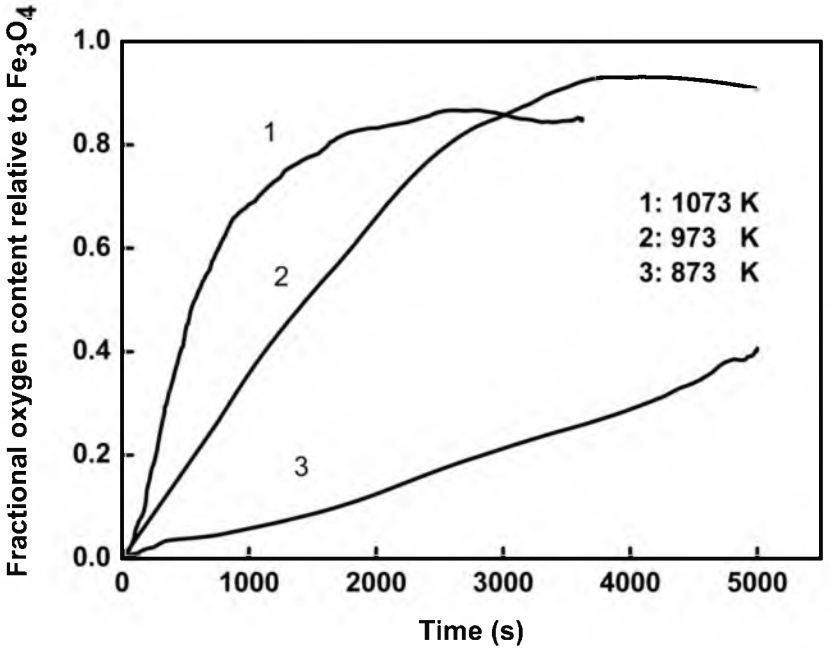

Fig. 41 Effect of temperature on reoxidation rate; 100% CO_2, P_{total} = 86.1 *kPa*

CHAPTER 4

CONCLUSIONS

A novel flash ironmaking process that directly reduces iron oxide concentrate particles is under development. As the product iron cools down in the lower part of the flash reactor, conditions may become favorable for reoxidation in H_2O and CO_2 because of equilibrium and high reactivity of iron particles. Flash reduced iron may also come into contact with air at moderate temperatures during transportation. The possibility of reoxidation of iron particles in various gas mixtures was investigated. The following conclusions are reached:

1) The nucleation and growth kinetics expression was found to describe the reoxidation of flash reduced iron particles in H_2O-H_2 and O_2-N_2 gas mixtures after detailed calculations and microstructure examination of the oxidized samples.
2) The oxidation reactions of flash reduced iron particles in H_2O-H_2 and O_2-N_2 gas mixtures both have first order dependence on the partial pressures of, respectively, water vapor and oxygen.
3) The activation energy of oxidation of flash reduced iron particles in H_2O-H_2

and O_2-N_2 gas mixtures are, respectively, 146 kJ/mol and 14.4 kJ/mol, which implies the former has greater temperature dependence than the latter.

4) Complete rate equations that adequately represent the experimental data were developed for oxidation in H_2O-H_2 and O_2-N_2 gas mixtures.

5) Reoxidation of flash reduced iron particles in pure CO_2 was slow compared with in H_2O and O_2 and it will not be of concern, whether in the suspension reduction process or in the iron product collector, especially considering CO_2 accounts for less than 10% of the gas mixture from the partial combustion of natural gas.

6) Iron particles flash reduced at temperatures 1200 – 1400 °C have close round microstructures and similar oxidation kinetics.

7) Flash reduced iron particles are much less vulnerable to oxidation than conventional direct reduced iron particles, because the novel flash ironmaking process uses higher reduction temperatures, leading to lower specific surface area.

8) The findings in the present work indicate that within several seconds of residence time typically available in a flash reduction process the reoxidation degree of iron particles in water vapor is < 0.24 % at the temperature range of 823 – 973 K (550 – 700 °C). In the collector where product iron particles may be kept for up to one hour at around 673 K (400 °C), the expected reoxidation degree is around 0.02 %. To further reduce oxidation in the product collector, an

inert gas device could be installed to dilute or prevent contact of oxidizing gas. In long distance transportation, it is advisable to make briquettes of flash reduced iron particles and prevent contact with air or moisture as much as possible.

APPENDIX A

EVALUATION OF EXTERNAL MASS TRANSFER'S EFFECT

A situation is considered where water vapor flows in a tubular reactor (2.54 cm inner diameter) over the sample holder (8 cm length and 1.2 cm width) at the temperature of 873K and a flow rate of 6 L/min (total pressure = atmospheric pressure in Salt Lake City = 86.1 kPa). The concentration gradient of water vapor over the sample holder is illustrated in Figure 42.

The oxidation reaction is

$$Fe + H_2O(g) = FeO + H_2(g) \qquad \text{(A-1)}$$

The average mass transfer coefficient for flow over a flat plate[43] is

$$k = 0.664 \cdot D_{AB} \cdot Sc^{1/3} / L \cdot Re^{1/2} \qquad \text{(A-2)}$$

where D_{AB} is a binary gas phase diffusion coefficient, m^2/s, Sc is the Schmidt number, L is the length of the flat plate (ceramic boat in this research), m, and Re is the Reynolds number of water vapor flow over the ceramic boat.

The Reynolds number

$$Re = \rho UL / \mu \qquad \text{(A-3)}$$

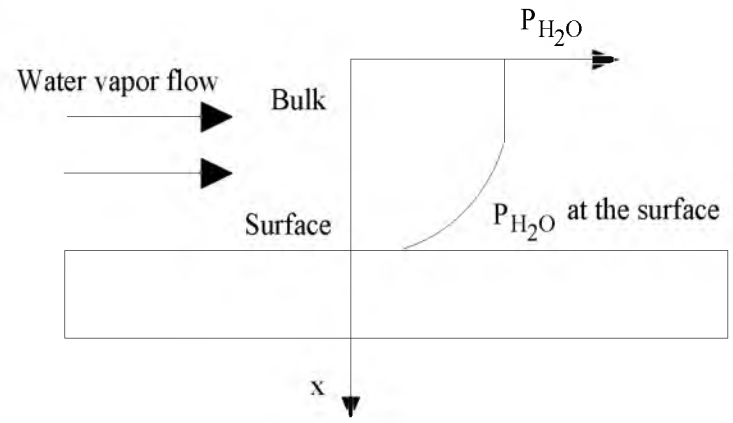

Fig. 42 Concentration gradient of water vapor over the sample holder

in which ρ is the density of water vapor at 873 K, *kg/m*^{3}, U is the linear velocity of water vapor, *m/s*, and μ is the viscosity of water vapor, *kg/m.s*.

$$\rho_{H_2O} = 0.214 \text{ kg/m}^3 \tag{A-4}$$

$$U = \frac{6\times10^{-3} m^3/min \times 1 min/60s}{\pi \times (0.0254/2)^2 m^2} = 0.2 m/s \tag{A-5}$$

According to Hines[43], the viscosity of water vapor at 873 K is

$$\mu = 3.25 \times 10^{-5} \text{ kg/m·s} \tag{A-6}$$

Hence,

$$Re = 105.4 \tag{A-7}$$

The Fuller-Schettler-Giddings[44] method is used to estimate the gas phase diffusion coefficient, expressed by

$$D_{H_2O-H_2} = \frac{1.00\times10^{-7} \cdot T^{1.75} \cdot \left(1/M_{H_2O} + 1/M_{H_2}\right)^{1/2}}{P \cdot \left[\left(\Sigma\nu_{H_2O}\right)^{1/3} + \left(\Sigma\nu_{H_2}\right)^{1/3}\right]^2} \tag{A-8}$$

where M_{H_2O} and M_{H_2} are, respectively, the molar mass of water vapor and hydrogen, *g/mol*, P is the pressure of the system (0.85 atm in Salt Lake City), T is the temperature, *K*, ν_{H_2O} and ν_{H_2} are, respectively, the atomic diffusion volumes of water vapor and hydrogen.

Using the correlation of Fuller-Schettler-Giddings[44], the values of atomic diffusion volumes of $\Sigma\nu$ are

$$\Sigma\nu_{H_2O} = 12.7 \tag{A-9}$$

$$\Sigma\nu_{H_2} = 7.07 \tag{A-10}$$

Temperature T = 873 K, pressure P = 0.85 atm, molecular weights M_{H_2O} = 18 g/mol; M_{H_2} = 2 g/mol. Substituting all the parameters into the equation yields the diffusion coefficient of the gas phase

$$D_{H_2O-H_2} = 6.8 \times 10^{-4}\ \mathrm{m^2/s} \tag{A-11}$$

The Schmidt number

$$Sc = \mu / \left(\rho \cdot D_{H_2O-H_2}\right) \tag{A-12}$$

in which,

$$\mu = 3.25 \times 10^{-5}\ kg/m \cdot s \tag{A-13}$$

$$\rho = 0.214\ \mathrm{kg/m^3} \tag{A-14}$$

$$D_{H_2O-H_2} = 6.8 \times 10^{-4}\ \mathrm{m^2/s} \tag{A-15}$$

Therefore,

$$Sc = 0.223 \tag{A-16}$$

Therefore, external mass transfer coefficient is

$$k = 0.664 \times \frac{6.8 \times 10^{-4} \times (0.223)^{1/3}}{0.08} 105.4^{1/2} = 0.035 m/s \tag{A-17}$$

The reaction in consideration is,

$$\mathrm{Fe + H_2O(g) = FeO + H_2(g)} \tag{A-18}$$

Assume the reaction is at equilibrium,

$$K_{873K} = 2.88 = \frac{p_{H_2,e}}{p_{H_2O,e}} \tag{A-19}$$

$$p_{H_2,e} + p_{H_2O,e} = 0.85 atm \tag{A-20}$$

Therefore, the partial pressure differences between the bulk and the surface of the plate is

$$\Delta p_{H_2O} = p_{H_2O,bulk} - p_{H_2O,e} = 0.63 \ \ atm \tag{A-21}$$

This is equal to a concentration gradient of

$$\Delta C_{H_2O} = 8.8 \ mol/m^3 \tag{A-22}$$

The area of the flat plate is

$$A = 0.08 \times 0.012 = 9.6 \times 10^{-4} \ m^2 \tag{A-23}$$

Hence, the calculated external mass transfer rate is

$$R_{cal} = k \cdot A \cdot \Delta C_{H_2O} = \ 2.9 \times 10^{-4} \text{ moles of } H_2O/s \tag{A-24}$$

The measured rate at the initial stage of experiments conducted at 973 K (700 °C) is

$$R_{exp.} = 2.7 \times 10^{-7} \text{ moles of } H_2O/s \tag{A-25}$$

The calculated external mass transfer rate is much faster than the measured rate, thus it can be concluded the measured rate is not affected by the external mass transfer.

APPENDIX B

EVALUATION OF INTERPARTICLE DIFFUSION'S EFFECT

Whether interparticle diffusion has a significant effect on the overall rate of a gas solid can be assessed by comparing the diffusion controlled rate with the experimentally observed rate. In the reaction investigated in this work, water vapor diffuses through a porous layer of iron particles, as illustrated in Figure 43, and undergoes the following reaction:

$$Fe + H_2O(g) = FeO + H_2(g) \qquad \text{(B-1)}$$

The relationship between conversion and time under interparticle diffusion control in a flat geometry is given by[26]

$$X^2 = \frac{K}{1+K}\left(C_{H_2O_b} - \frac{C_{H_{2b}}}{K}\right)\frac{2bD_e}{(1-\in)\rho_s}\left(\frac{A_p}{F_pV_p}\right)^2 t \qquad \text{(B-2)}$$

where t is the reaction time, X is the fractional conversion of the solid, K is the equilibrium constant of the reaction of interest, b is the stoichiometry coefficient of reaction (= 1 for the reaction in question), F_p = 1, D_e is the effective gas phase diffusion coefficient, $\in$ is the voidage of the particle bed, $(1-\in)\rho_s$ is the number of moles of solid reactant per unit volume of the bed, V_p and A_p are, respectively, the

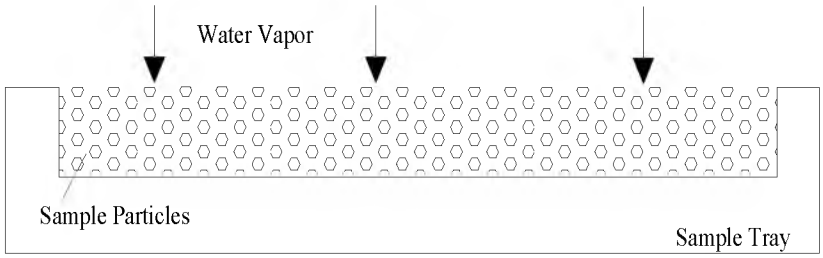

Fig. 43 Illustration of water vapor diffusing through a porous layer of iron particles

volume and surface area of the particle layer, $C_{H_2O_b}$ and $C_{H_{2b}}$ are, respectively, the bulk molar concentration of water vapor and hydrogen. The time needed to reach complete conversion is

$$t_{X=1} = \frac{1+K}{K}\frac{(1-\in)\rho_s\left(V_p / A_p\right)^2}{2D_e\left(C_{H_2O_b} - C_{H_{2b}} / K\right)} = \frac{1+K}{K}\frac{(1-\in)\rho_s L_p{}^2}{2D_e\left(C_{H_2O_b} - C_{H_{2b}} / K\right)} \quad \text{(B-3)}$$

where L_p is the thickness of the particle layer. The equilibrium constant of reaction (B1) at 873 K is

$$K = 2.88 \quad \text{(B-4)}$$

Molar density of iron particles is

$$\rho_s = 0.14 \text{ mol/cm}^3 \quad \text{(B-5)}$$

The voidage of iron particle bed of 100 mg with an area of 9 cm^2 and thickness of 0.5 mm is

$$\in = 0.97 \quad \text{(B-6)}$$

and

$$V_p/A_p = L_p \quad \text{(B-7)}$$

Consider in the gas mixture, p_{H_2O} / p_{H_2} = 80%/20%, (P_{total} = 86.1 kPa),

$$C_{H_2O_b} - C_{H_{2b}} / K = 8.66\times10^{-6} \text{ mol/cm}^3 \quad \text{(B-8)}$$

According to the Fuller-Schettler-Giddings[44] method, the gas phase diffusion coefficient can be obtained from the following relationship:

$$D_{H_2O-H_2} = \frac{1.00\times10^{-7}\cdot T^{1.75}\cdot\left(1/M_{H_2O}+1/M_{H_2}\right)^{1/2}}{P\cdot\left[\left(\Sigma\nu_{H_2O}\right)^{1/3}+\left(\Sigma\nu_{H_2}\right)^{1/3}\right]^2} \quad \text{(B-9)}$$

$$D_e = D\cdot\in^2 \quad \text{(B-10)}$$

where T = 873 K, total pressure P = 0.85 atm, molecular weights M_{H_2O} = 18 g/mol, M_{H_2} = 2 g/mol, ν_{H_2} = 7.07, and ν_{H_2O} = 12.7.

Substitute all known variables to get

$$D_e = 6.4 \text{ cm}^2/\text{s} \quad \text{(B-11)}$$

Therefore,

$$t_{X=1} = \frac{1+K}{K}\frac{(1-\in)\rho_s\left(V_p/A_p\right)^2}{2D_e\left(C_{H_2O_b}-C_{H_{2b}}/K\right)}$$

$$= \frac{1+2.88}{2.88}\frac{(1-0.97)\times0.14\left(L_p\right)^2}{2\times6.4\times8.66\times10^{-6}} \quad \text{(B-12)}$$

According to the above equation, if the thickness of sample layer is 0.05 cm, the time required for the reaction to reach completion is 0.13 second. However, the observed rate was much slower than this calculated rate. Thus, it can be concluded that the reaction rate was not affected by the inter particle diffusion.

REFERENCES

1. H. Y. Sohn, M. E. Choi, Y. Zhang, and J. E. Ramos: *Iron Steel Technol. (AIST Trans.)*, 2009, vol. 6, pp. 158-65.

2. M. E. Choi: Ph.D. Dissertation, University of Utah, Salt Lake City, Utah, May 2010.

3. H. Y. Sohn: *Steel Times International*, 2007, vol. 31, pp. 68-72.

4. J. Szekely, and N. J. Themelis: *Rate Phenomena in Process Metallurgy*, Wiley–Interscience, New York, 1971, pp. 606-08.

5. M. E. Choi, H. Y. Sohn, G. Han: in *2006 Sohn International Symposium*, San Diego, CA, Aug 26, 2006.

6. Michael G. King: *JOM*, 2007, vol. 59, pp.21-27.

7. W. G. Davenport and E. H. Partelpoeg: *Flash Smelting: Analysis, Control and Optimization*. Pergamon Press, New York, 1987, pp. 20-35.

8. W. G. Davenport, M. King, M. Schlesinger, and A.K. Biswas. *Extractive Metallurgy of Copper*. 4th Edition, Elsevier Science Ltd, Oxford, 2002, pp. 73-102.

9. H. Y. Sohn, M. E. Choi, M. Olivas-Martinez, and H.G. Kim: *Proceedings of Cleantech 2011*, Hungary International Conference on Clean Technologies in the Steel Industry, Budapest, Hungary, September 26-28, 2011

10. Outokumpu HSC Chemistry 5.1 for Windows – Chemical Reaction and Equilibrium Software with Extensive Thermochemical Database, Pori, Finland: Outokumpu Research Oy.

11. R. L. Stephenson. *Direct Reduced Iron: Technology and Economics of Production and Use*. The Iron and Steel Society of AIME, Warrendale, PA,

1980, pp. 64-99

12. E. T. Turkdogan, W. M. McKenwan, and L. Zwell: *J. Physical Chemistry*, 1965, vol. 69, pp. 327-34

13. H. Yin, W. Y. D. Yuen and D. J. Young: *Mater. Corros.*, 2012, vol. 63, pp. 869-77

14. A. A. El-Geassy, F. O. El-Kashif, M. I. Nasr, and A. A. Omar: *ISIJ Int.*, 1994, vol. 34, pp. 541-47.

15. A. Bandopadhyay, A. Ganguly, K. K. Prasad, S. B. Sarkar, and H. S. Ray:*ISIJ Int.*, 1989, vol. 29, pp. 753-60.

16. A. Bandopadhyay, A. Ganguly, K. K. Prasad, S. B. Sarkar, and H. S. Ray: *Thermochim. Acta*, 1993, vol. 228, pp. 271-81.

17. A. Bandopadhyay, A. Ganguly, K. K. Prasad, S. B. Sarkar, and H. S. Ray: *React. Solids*, 1990, vol. 8, pp. 77-89.

18. A. Bandopadhyay, A. Ganguly, K. N. Gupta, and H. S. Ray: *Thermochim. Acta*, 1996, vol. 276, pp. 199-207.

19. P. Kaushik and R. J. Fruehan: *Metall. Mater. Trans. B*, 2006, vol. 37B, pp. 715-25.

20. P. Kaushik and R.J. Fruehan: *Metall. Mater. Trans. B*, 2006, vol. 37B, pp.727-32.

21. W. R. Schütze: HBI – Hot Briquetting of Direct Reduced Iron Technology and Status of Industrial Application, Maschinenfabrik Köppern GmbH & Co. KG, Hattingen, Germany, 1999.

22. M. E. Choi and H. Y. Sohn: *Ironmaking Steelmaking,* 2010, vol. 37, pp. 81-88.

23. H. Wang and H. Y. Sohn: *Metall. Mater. Trans. B*, 2013, vol. 44, pp. 133-45.

24. International Organization for Standardization, Direct Reduced Iron - Determination of Metallic Iron-Bromine-Methanol Titrimetric Method, *ISO 5416*, 3rd edition, Geneva, Switzerland: ISO, 2006.

25. Electrochemical Society, Iron Ore Reduction: Proceedings of a Symposium of

the Electrothermics and Metallurgy Division of the Electrochemical Society, R. R. Rogers ed., Pergamon Press, Chicago, 1962. pp. 208-09

26. J. Szekely, J. W. Evans, and H. Y. Sohn: *Gas–Solid Reactions*, Academic Press, New York, 1976, pp. 73–81, 131.

27. H. Wang: Ph.D. Dissertation, University of Utah, Salt Lake City, Utah, May 2011.

28. S. Seetharaman and H. Y. Sohn: *Fundamentals of Metallurgy,* S. Seetharaman, ed., Woodhead Publishing Limited, Cambridge, U.K., 2005, pp. 299-310.

29. N. J. Themelis and W. H. Gauvin: *Trans. Am. Inst. Min. Metall. Pet. Eng.*, 1963, vol. 227, pp. 290-300.

30. S. K. El-Rahaiby and Y. K. Rao: *Metall. Mater. Trans. B*, 1979, vol. 10B, pp. 257-69.

31. P. C. Hayes: *Metall. Mater. Trans. B*, 1979, vol. 10B, pp. 211-17.

32. M. E. Choi, H. Y. Sohn, Y. M. Z. Ahmed, F. M. Mohamed, G. Han, and M. E. H. Shalabi: *Chem. Eng. Technol.,* 2007, vol. 30, pp. 628-34.

33. M. Avrami: *J. Chem. Phys.*, 1939, vol. 7, pp. 1103–1112.

34. M. Avrami: *J. Chem. Phys.*, 1940, vol. 8, pp. 212–24.

35. M. Avrami: *J. Chem. Phys.*, 1941, vol. 9, pp. 177–84.

36. IUPAC: *Compendium of Chemical Terminology*, 2nd ed., Compiled by A.D. McNaught and A. Wilkinson, Blackwell Scientific Publications, Oxford, 1997, p. 85.

37. W. A. Johnson and R. F. Mehl:, *TMS-AIME*, 1939, vol. 135, pp. 416-58.

38. P. W. M. Jacobs and F. C. Tompkins: Classification and Theory of Solid Reactions In: *Chemistry of the Solid State*, W. E. Garner, *ed.*, Butterworths, London, 1955, pp. 184-212.

39. W. W. Smeltzer: *Acta Metall.*, 1960, vol. 8, pp. 377-83.

40. H. Pfeiffer and C. Laubmeyer: *Zeitschrift Elektrochemie*, 1955, vol. 59, pp.

579-83.

41. W. E. Boggs, R. H. Kachik and G. E. Pellissier: *J. Electrochem. Soc.,* 1965, vol. 112, pp. 539-46

42. B.-S. Kim and H. Y. Sohn: *Metall. Mater. Trans. B*, 2002, vol. 33B, pp. 717-21.

43. A. L. Hines, R. N. Maddox, *Mass Transfer Fundamentals and Applications*, Prentice Hall, New Jersey, 1984, pp. 185, 501

44. E. N. Fuller, P. D. Schettler, and J. C. Giddings: *Ind. Eng. Chem.,* 1966, vol. 58, pp. 18-27.